LA-UR-21-30049
Approved for public release; distribution is unlimited.

Title: (U) Updated Godiva-IV Benchmark Preview

Author(s): Favorite, Jeffrey A.

Intended for: Report

Issued: 2021-10-11

Los Alamos
NATIONAL LABORATORY
memorandum
X-Computational Physics Division
Radiation Transport Applications Group
Group XCP-7, MS F663
Los Alamos, New Mexico 87545
505/667-1920

To/MS: Distribution
From/MS: Jeffrey A. Favorite / XCP-7, MS F663
Phone/Email: 7-7941 / fave@lanl.gov
Symbol: XCP-7:21–017(U) (LA–UR–21–????)
Date: October 7, 2021

SUBJECT: (U) Updated Godiva-IV Benchmark Preview

Abstract—A note of errata prepended to the Godiva-IV delayed-critical benchmark (HEU-MET-FAST-086) identifies two corrections that need to be made to the model: The glory hole in the spindle should be made larger, and the height of the safety block should be made smaller (and therefore its density made larger). In addition, the safety block at its full-in position is closer to the inner subassembly plate than was modeled in the benchmark. These changes have been made to HEU-MET-FAST-086 Case 4 in order to estimate the effect on k_{eff} and on the neutron flux spectrum. Using smaller separation, a smaller safety block, and a larger glory hole caused k_{eff} to increase by 453 ± 1 pcm from the benchmark. The latest nuclear data, ENDF-B/VIII.0, have also been used; this caused k_{eff} to increase another 37 ± 1 pcm. Flux spectra were compared in a modeled fission foil and at three external point detectors. Within the fission foil, using ENDF/B-VIII.0 for Godiva-IV induced changes in the flux spectrum similar in size to the changes due to using smaller separation, a smaller safety block, and a larger glory hole. At the point detectors, using ENDF/B-VIII.0 induced changes in the flux spectrum much larger than those due to changing the model. In other words, the corrections to the benchmark model cause a large increase in k_{eff}, but the changes to the neutron flux spectrum are small compared to those caused by using the latest nuclear data. This study presents a preview of results expected during the reevaluation of the Godiva IV benchmark, but it is not a substitute for the full reevaluation.

I. Introduction

After the release of the Godiva-IV ICSBEP delayed-critical benchmark[1] (HEU-MET-FAST-086), an errata note was issued that listed two corrections to be made to the model: The glory hole in the spindle should be made larger, and the height of the safety block fuel should be reduced to account for the presence of a metal shim. (This affects the calculated density of the safety block). In addition, the separation between the top of the safety block and the inner subassembly plate was modeled as 0.1 inches for all cases, which was too large by a factor of 10. Correcting these issues would make the Godiva-IV benchmark models consistent with the assembly as it existed at TA-18. Since moving to Building 302 at the Device Assembly Facility (DAF), the separation distance is slightly larger. A new benchmark evaluation of Godiva-IV in Building 302 is needed both to incorporate the corrections and to provide a baseline for the current location within a smaller building.

In the meantime, the Godiva-IV benchmark model was modified to match the current configuration with the latest nuclear data in order to assess the effect of the changes on reactivity and spectral characteristics from the benchmark. Calculations were done with a version of MCNP6.2 (Ref. 2) that was slightly modified to print more digits for tally relative uncertainties.

The next section of this report calculates k_{eff} and spectral parameters for HEU-MET-FAST-086 Case 4 using the production release of ENDF/B-VII.1 nuclear data. In Sec. III, the diameter of the glory hole in the spindle is increased. In Sec. IV, the height of the safety block is decreased and its density is increased. In Sec. V, the separation between the safety block and the inner subassembly plate is decreased. In Sec. VI, a model for Building 302 is introduced. The modifications of Secs. III through VI are cumulative. In Sec. VII, the model of Sec. V is run with ENDF/B-VIII.0 nuclear data. Section VIII provides a summary and conclusions. Appendix A discusses the calculation of the Godiva-IV fission conversion factor. Appendix B lists two input files.

II. Production Release of ENDF/B-VII.1

Sample calculations in HEU-MET-FAST-086 Section 4 used a version of ENDF/B-VII.1 nuclear data that may have been preliminary. The reported k_{eff} for Case 4 was 0.9907 ± 0.0003. Results from a higher-precision calculation with the production release are reported in Table I. k_{eff} is 47 ± 30 pcm larger (all k_{eff}'s reported in this paper are the average of three independent values). The average neutron energy causing fission (ANEF) and energy corresponding to the average neutron lethargy causing fission (EALF) are also reported in Table I along with the fraction of fissions caused by neutrons in the thermal (< 0.625 eV), intermediate (0.625 eV - 100 keV), and fast (>100 keV) energy ranges.

The Godiva-IV fission conversion factor was computed using an HEU foil with diameter 0.2220 inches, thickness 0.00248 cm, density 18.5994 g/cm^3, and ^{235}U concentration 93.3022 wt% (using MCNP atomic weights and Avogadro's number, not ICSBEP values). The bottom of the foil was 0.43425 cm above the bottom of the inner subassembly plate. The sample holder was pure ^{27}Al with a density of 2.62524 g/cm^3; its inner and outer radii were 0.284791 and 0.311297 cm. This model was based on a real fission foil that was irradiated and counted during Godiva-IV startup at the DAF. See Appendix A for the details of the fission conversion factor calculation.

Table I. Godiva-IV Results Using Production Release of ENDF/B-VII.1.

Parameter		Value
k_{eff}		0.99117 ± 0.00001
ANEF		1.4271 MeV
EALF		0.79836 MeV
Fraction of fissions caused by neutrons in energy range	thermal	0.00 %
	intermediate	5.49 %
	fast	94.51 %
Fission conversion factor[(a)]		3.435E+4 ± 0.11%

(a) (Fissions in Godiva-IV)/[(Fissions in foil)/(g ^{235}U in foil)].

III. Increase Spindle Glory Hole Diameter

The spindle glory hole diameter was increased from 0.25 inches to 0.563 inches. The density of the spindle was not changed. Results from the modified model are shown in Table II. k_{eff} decreased by 62 ± 1 pcm from the result shown in Table I. The diameter of the fission foil was increased to 0.5 inches, and the inner and outer diameters of the sample holder were increased to 0.505 and 0.552 inches. (The fission foil and sample holder in Sec. II occupied the same fractional cross-sectional area of the glory hole as the fission foil and sample holder in this and subsequent sections.) Comparing Table II with Table I shows that increasing the spindle glory hole diameter causes a very slight hardening of the neutron spectrum within Godiva-IV.

Table II. Godiva-IV Results Using Larger Glory Hole and Production Release of ENDF/B-VII.1.

Parameter		Value
k_{eff}		0.99055 ± 0.00001
ANEF		1.4285 MeV
EALF		0.79934 MeV
Fraction of fissions caused by neutrons in energy range	thermal	0.00 %
	intermediate	5.48 %
	fast	94.52 %
Fission conversion factor[(a)]		3.431E+4 ± 0.05%

(a) (Fissions in Godiva-IV)/[(Fissions in foil)/(g ^{235}U in foil)].

IV. Decrease Height and Increase Density of Safety Block

The height of the safety block was decreased from 7.95728 cm to 7.49568 cm by raising the bottom. The change in height was –0.1016 cm or –0.040 inches. A 0.040-inch thick steel 1018 shim (outer radius 4.0005 cm, inner radius 1.27 cm, density 7.87 g/cm^3) was placed between the safety block and the pedestal of the safety block base. The density of the safety block was increased from 0.047100 atoms/(b·cm) to 0.047738 atoms/(b·cm) to preserve the safety block mass of 7276.0 g. These densities correspond to 18.1314 and 18.3770 g/cm^3, respectively (using MCNP atomic weights and Avogadro's number, not ICSBEP values). Results from the modified model are shown in Table III. k_{eff} increased by 81 ± 1 pcm from the result shown in Table I. This is well within the ±220-pcm uncertainty given for Case 4 in Table 27 of the benchmark.[1] Comparing Table III with Table I shows that decreasing the size of the safety block while increasing the spindle glory hole diameter has very little effect on the neutron spectrum within Godiva-IV.

Table III. Godiva-IV Results Using Smaller Safety Block, Larger Glory Hole, and Production Release of ENDF/B-VII.1.

Parameter		Value
k_{eff}		0.99198 ± 0.00001
ANEF		1.4279 MeV
EALF		0.79889 MeV
Fraction of fissions caused by neutrons in energy range	thermal	0.00 %
	intermediate	5.49 %
	fast	94.51 %
Fission conversion factor[(a)]		3.427E+4 ± 0.05%

(a) (Fissions in Godiva-IV)/[(Fissions in foil)/(g ^{235}U in foil)].

The flux spectrum in the fission foil in the modified model is compared with the flux spectrum in the fission foil in HEU-MET-FAST-086 (Sec. II) in Figure 1. The spectra in the top figure are very similar, but the bottom figure shows the difference, modified model minus HEU-MET-FAST-086 (note this is absolute, not relative). The largest differences occur around 3 MeV, where the relative difference is ~0.015/0.23 = 6.5%.

The flux spectra were also computed at three points around Godiva-IV. The point locations, given in Table IV, correspond approximately to points that were used in Ref. 3. The $z = 0$ plane is the bottom surface of the inner subassembly plate, and the intersection of the $x = 0$ and $y = 0$ planes is the Godiva-IV axis. When Building 302 is used in Sec. VI, the floor will be 173.01591 cm below the bottom surface of the inner subassembly plate, the x direction will be towards the closest wall, and the y direction will be away from the opening to the room.

Table IV. Point Detectors.

Index	*x* (cm)	*y* (cm)	*z* (cm)	Distance from axis (cm)	Height above floor (cm)
1	128.557522	153.208889	23.984090	200	197.0
2	219.406110	–204.599508	–3.515910	300	169.5
3	–142.042785	–373.930271	–50.015910	400	123.0

The flux spectra are compared for the three point detectors in Figure 2, Figure 3, and Figure 4. As in the fission foil (Figure 1), there is a slight hardening of the spectrum around 3 MeV, but in the point detectors it is much smaller, ~0.00045/0.25 = 0.18%.

All spectra in this report were computed using the standard LANL 250-group energy-bin structure.[4]

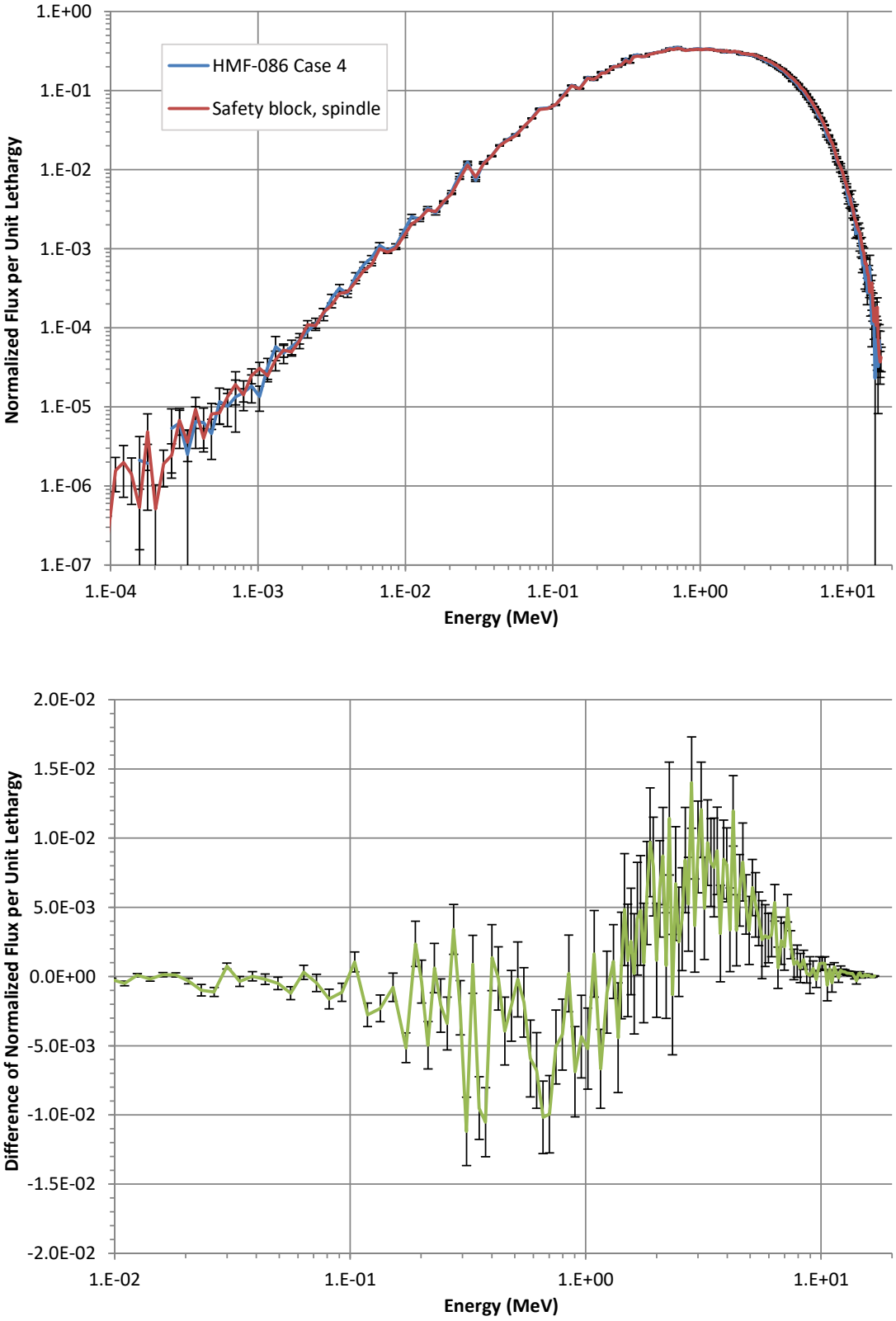

Figure 1. Comparison of neutron flux spectra in the fission foil between HEU-MET-FAST-086 and Godiva-IV using smaller safety block, larger glory hole, and production release of ENDF/B-VII.1.

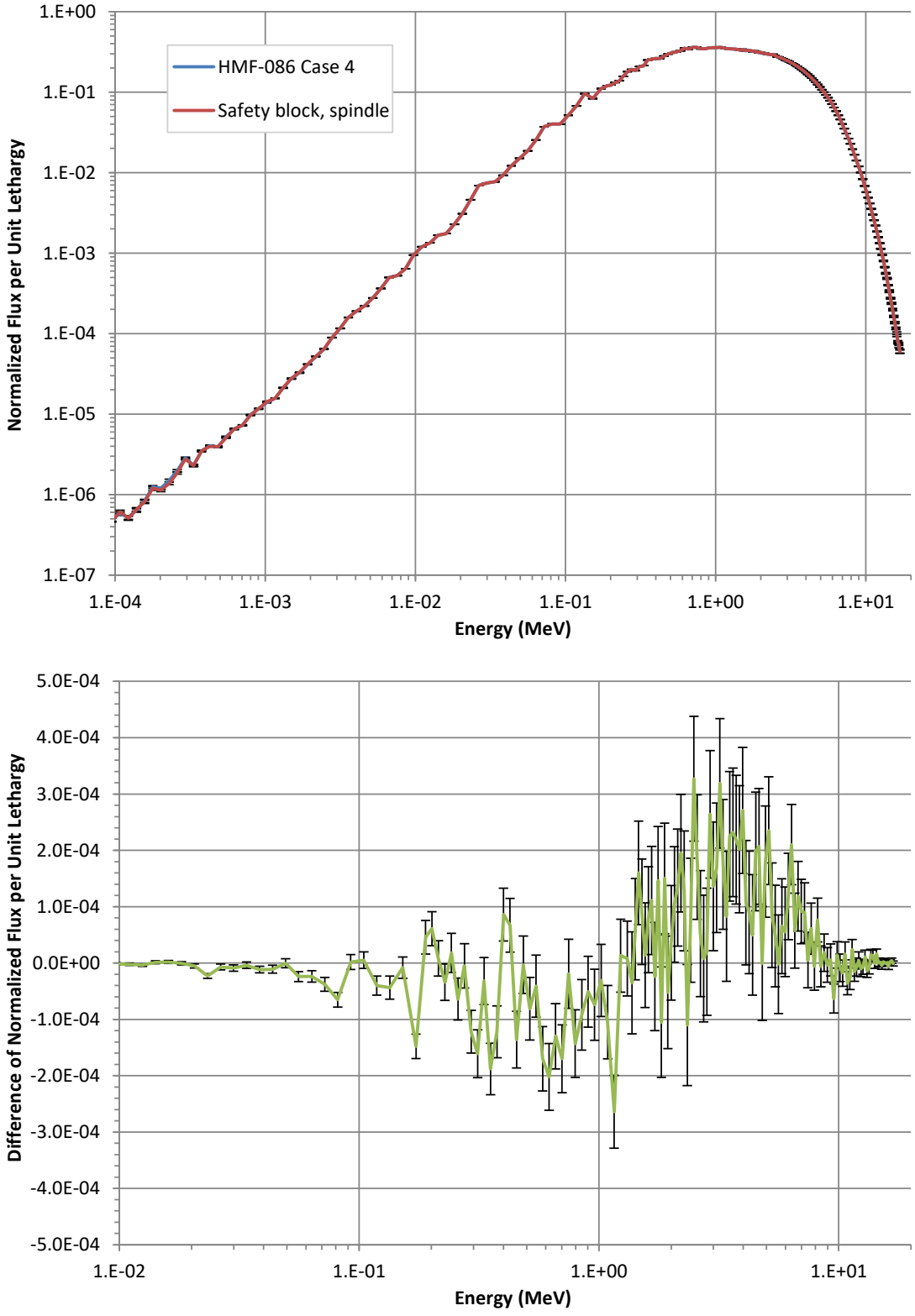

Figure 2. Comparison of neutron flux spectra at point detector 1 between HEU-MET-FAST-086 and Godiva-IV using smaller safety block, larger glory hole, and production release of ENDF/B-VII.1.

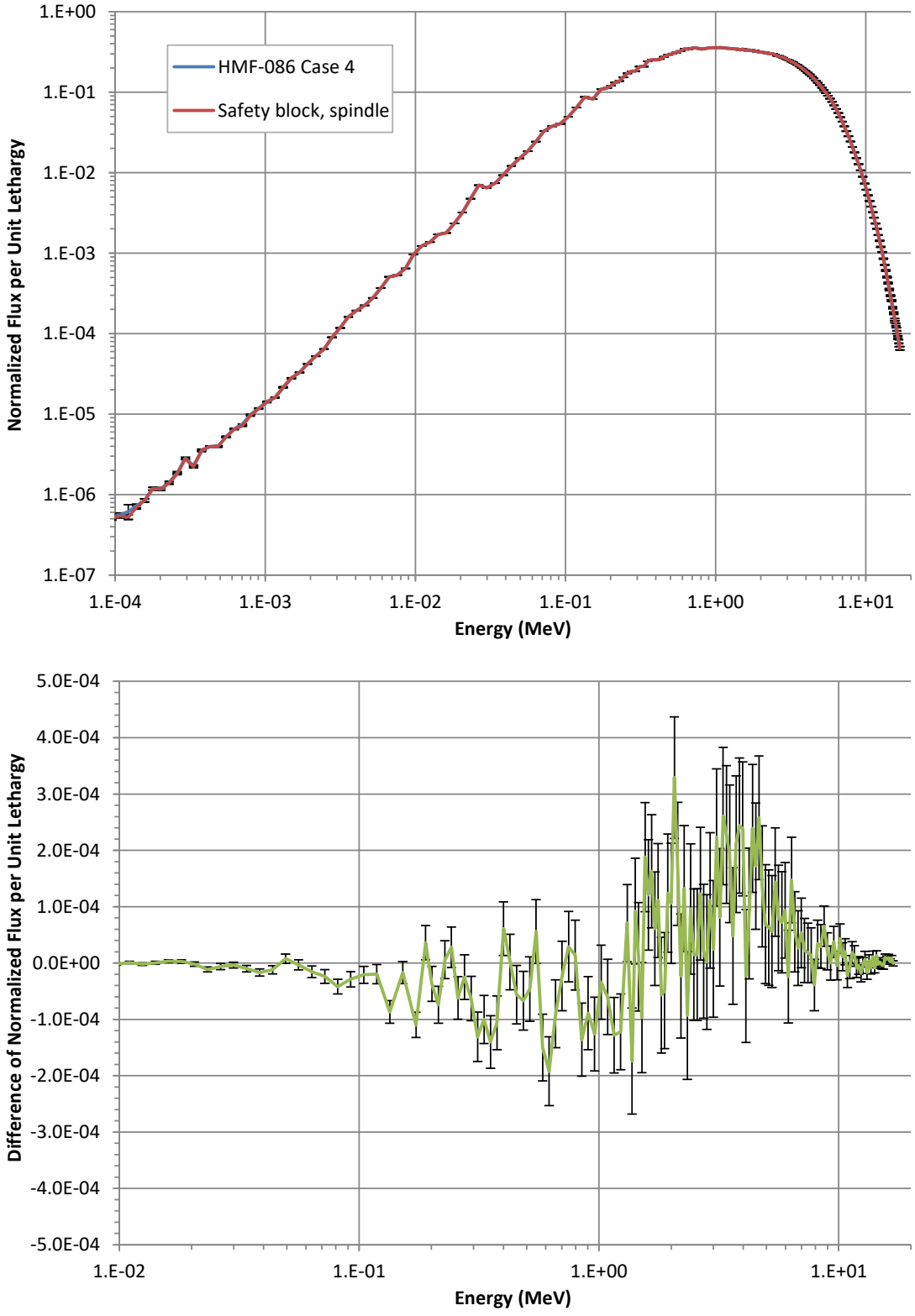

Figure 3. Comparison of neutron flux spectra at point detector 2 between HEU-MET-FAST-086 and Godiva-IV using smaller safety block, larger glory hole, and production release of ENDF/B-VII.1.

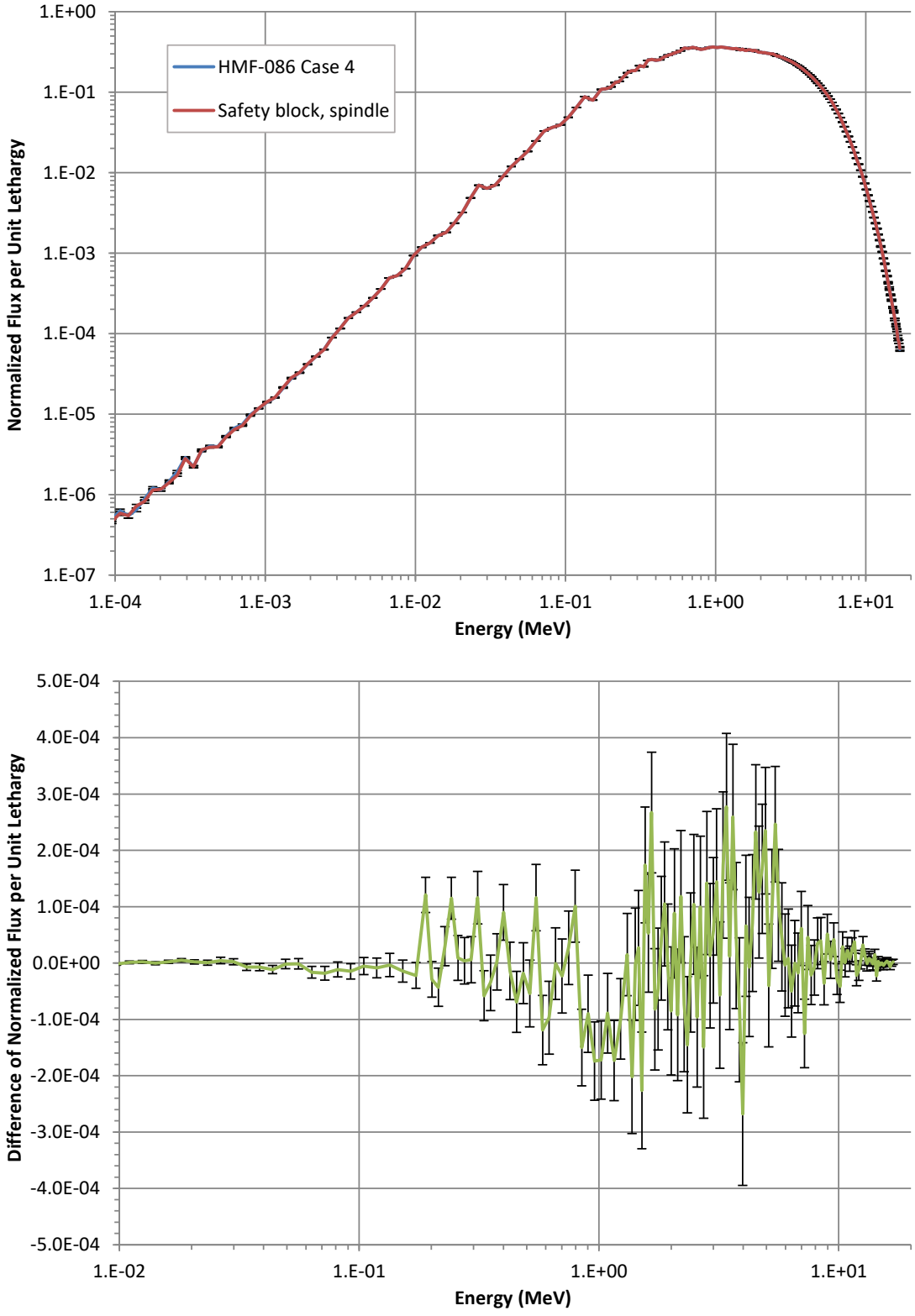

Figure 4. Comparison of neutron flux spectra at point detector 3 between HEU-MET-FAST-086 and Godiva-IV using smaller safety block, larger glory hole, and production release of ENDF/B-VII.1.

V. Decrease Separation Between Safety Block and Inner Subassembly Plate

During the reassembly of Godiva-IV in its new location (that is, new since the publication of HEU-MET-FAST-086) in Building 302 at the DAF, the separation between the safety block and the inner subassembly plate was measured to be between 0.0145 and 0.0175 inches. This is a better estimate of the separation at TA-18 than the 0.1 inches used in the benchmark. In the revised model, the separation was reduced from 0.1 inches to 0.0160 inches. Results from the modified model are shown in Table V. k_{eff} increased by 453 ± 1 pcm from the result shown in Table I. This is well outside the ±220-pcm uncertainty given for Case 4 in Table 27 of the benchmark.[1] Comparing Table V with Table I shows that decreasing the separation distance while decreasing the size of the safety block and increasing the spindle glory hole diameter causes a very slight softening of the neutron spectrum within Godiva-IV.

Table V. Godiva-IV Results Using Smaller Separation, Smaller Safety Block, Larger Glory Hole, and Production Release of ENDF/B-VII.1.

Parameter		Value
k_{eff}		0.99570 ± 0.00001
ANEF		1.4264 MeV
EALF		0.79774 MeV
Fraction of fissions caused by neutrons in energy range	thermal	0.00 %
	intermediate	5.50 %
	fast	94.50 %
Fission conversion factor[(a)]		3.357E+4 ± 0.05%

(a) (Fissions in Godiva-IV)/[(Fissions in foil)/(g ^{235}U in foil)].

The flux spectrum in the fission foil in the modified model is compared with the flux spectrum in the fission foil in HEU-MET-FAST-086 (Sec. II) in Figure 5. The spectra in the top figure are very similar, but the bottom figure shows the difference, modified model minus HEU-MET-FAST-086 (note this is absolute, not relative). As in Figure 1, the largest differences occur around 3 MeV, and the relative difference is about the same as in Figure 1.

The flux spectra are compared for the three point detectors in Figure 6, Figure 7, and Figure 8. Unlike in the fission foil (Figure 5), there are three areas with noticeable differences. The spectrum is larger at ~0.5 MeV and ~4 MeV, but smaller at ~2 MeV. Point detector 3 (Figure 8), which is furthest from the assembly, does not have the increase at 4 MeV.

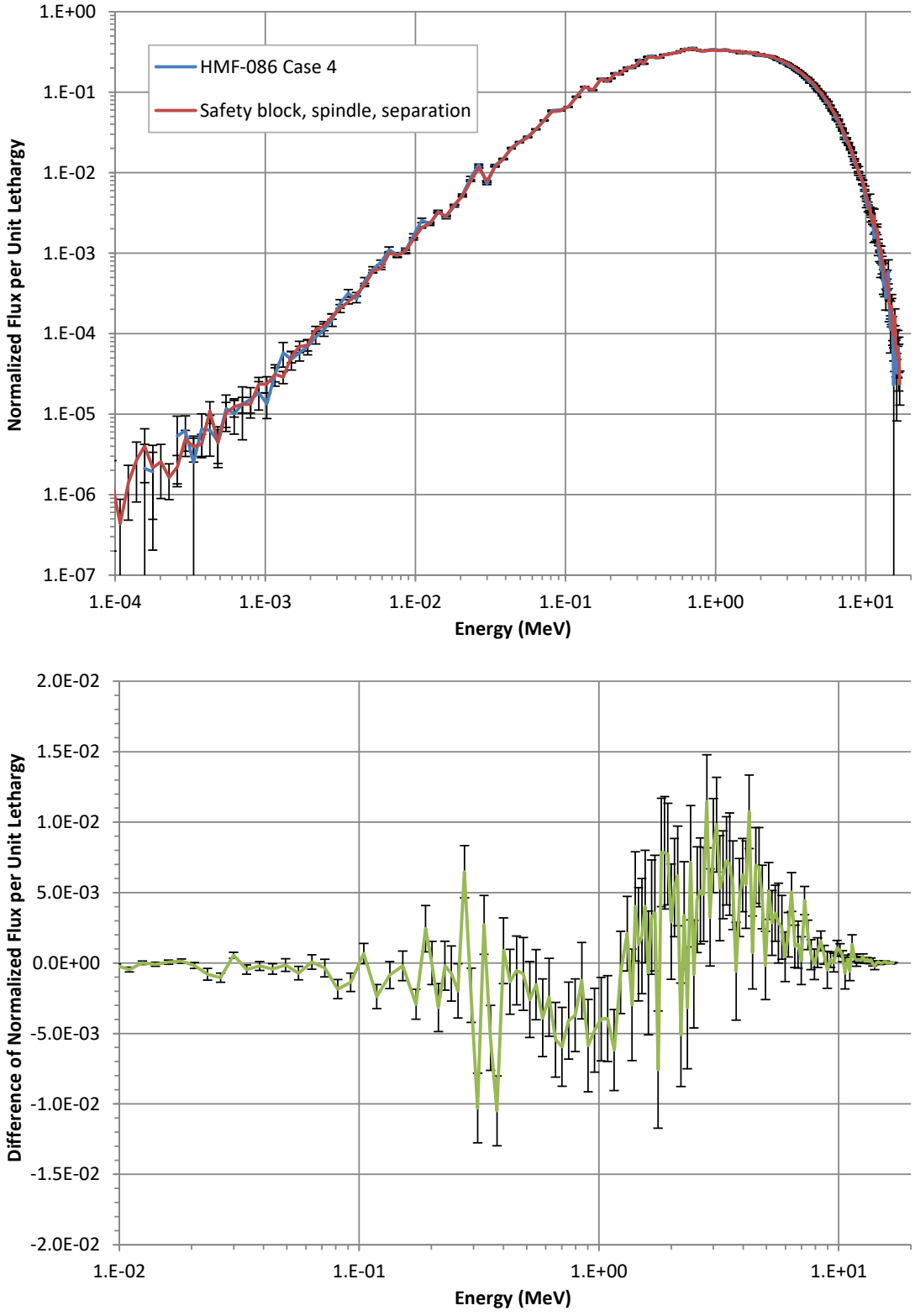

Figure 5. Comparison of neutron flux spectra in the fission foil between HEU-MET-FAST-086 and Godiva-IV using smaller separation, smaller safety block, larger glory hole, and production release of ENDF/B-VII.1.

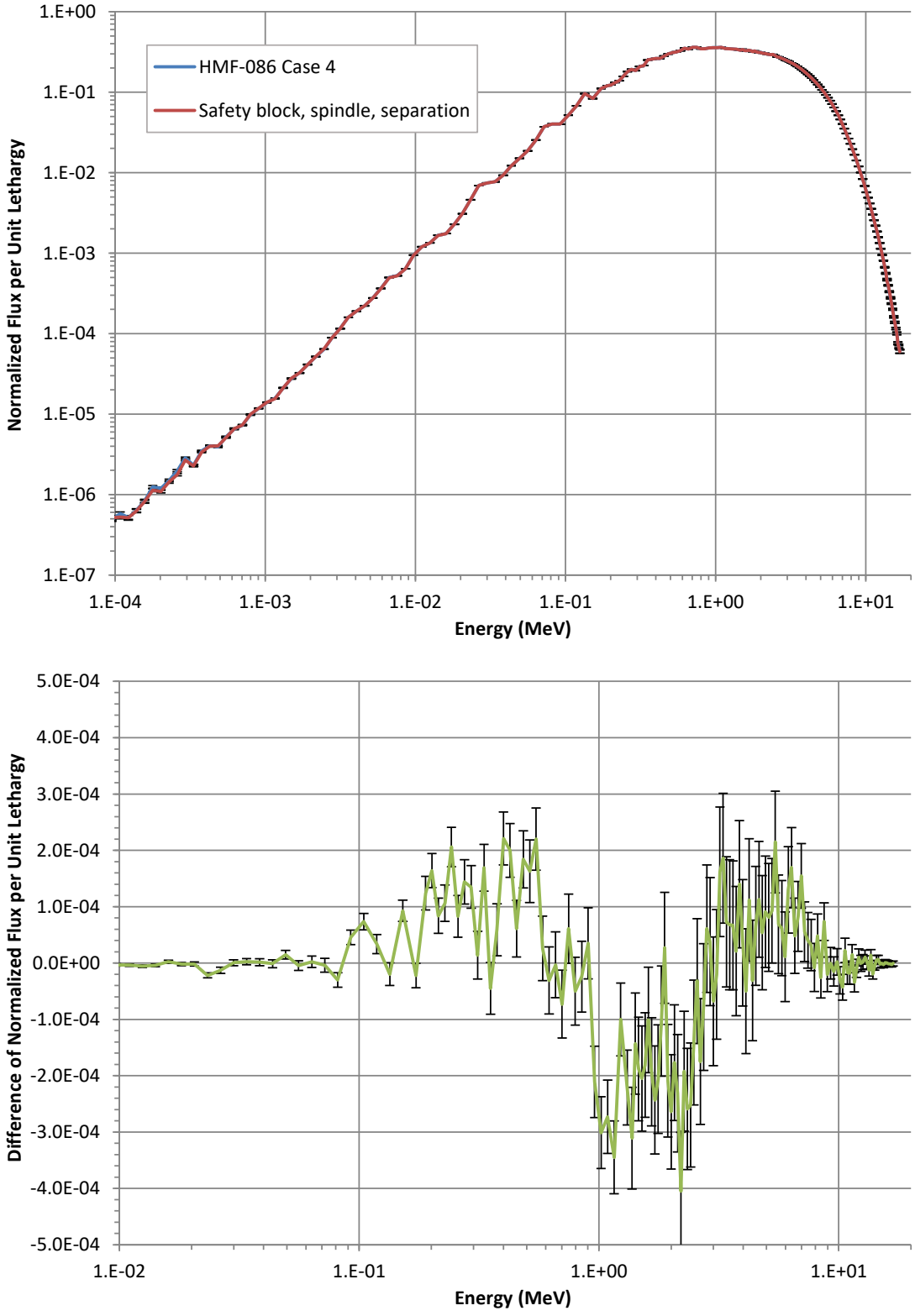

Figure 6. Comparison of neutron flux spectra at point detector 1 between HEU-MET-FAST-086 and Godiva-IV using smaller separation, smaller safety block, larger glory hole, and production release of ENDF/B-VII.1.

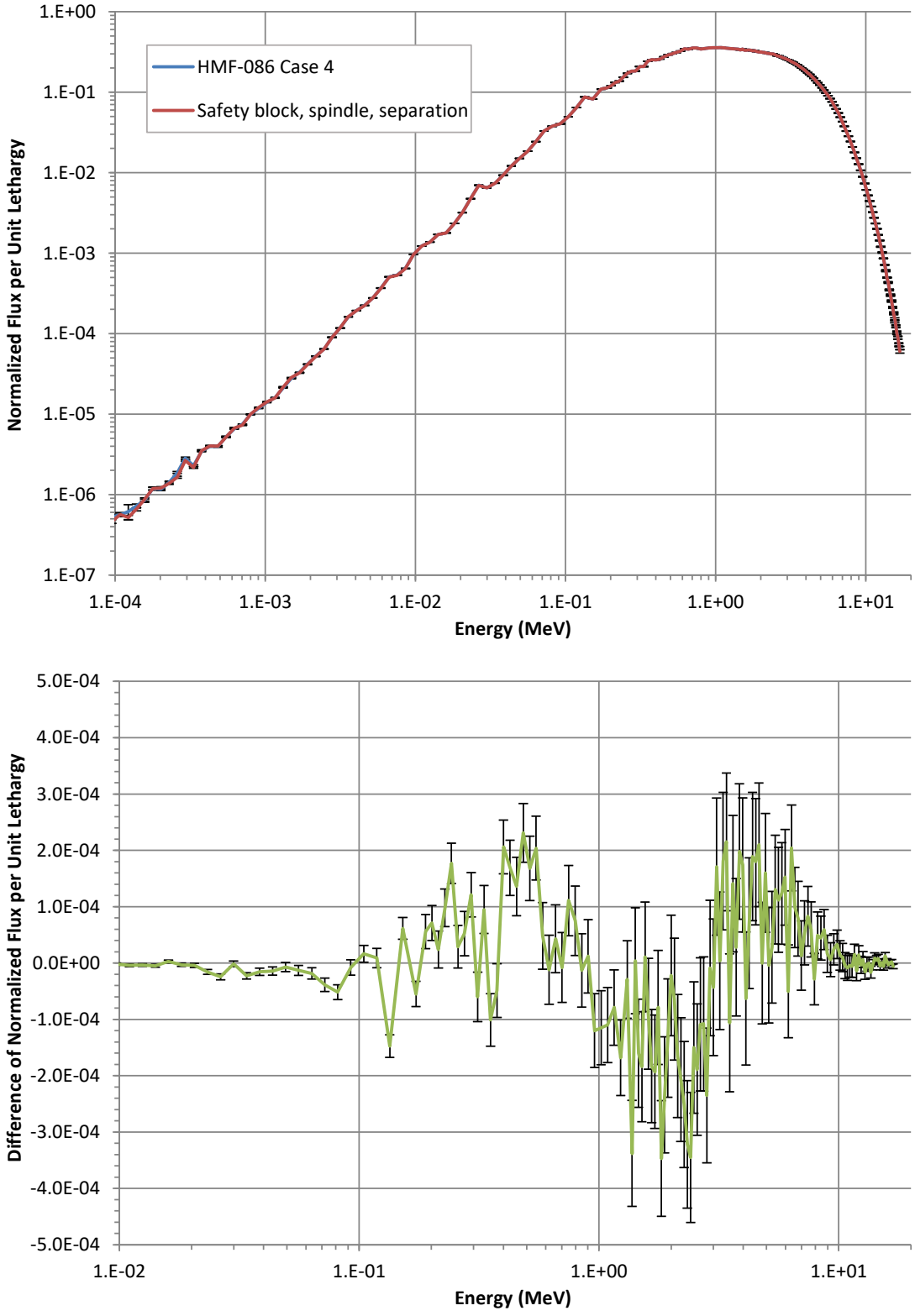

Figure 7. Comparison of neutron flux spectra at point detector 2 between HEU-MET-FAST-086 and Godiva-IV using smaller separation, smaller safety block, larger glory hole, and production release of ENDF/B-VII.1.

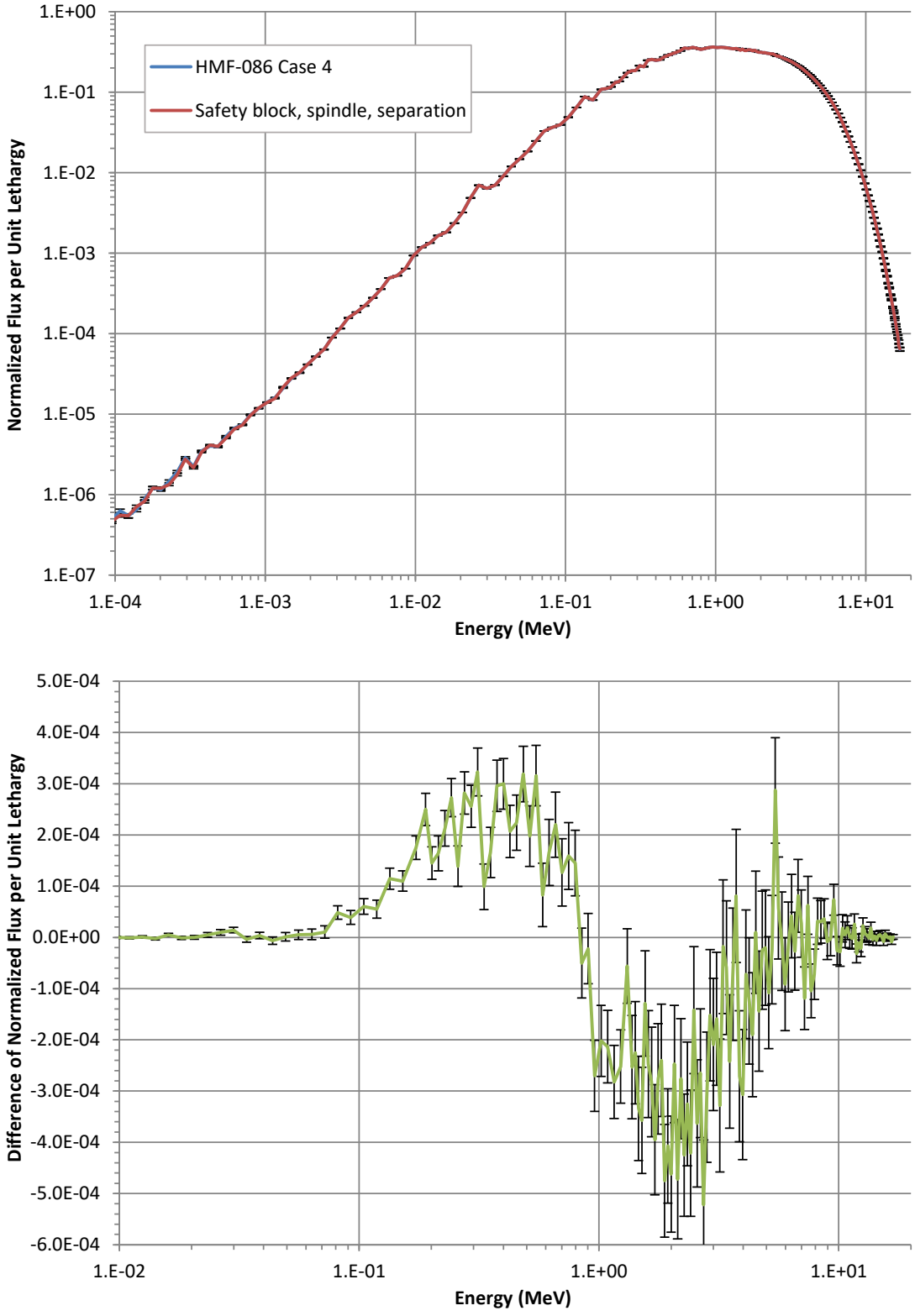

Figure 8. Comparison of neutron flux spectra at point detector 3 between HEU-MET-FAST-086 and Godiva-IV using smaller separation, smaller safety block, larger glory hole, and production release of ENDF/B-VII.1.

VI. Move to Building 302

Godiva-IV now resides in Building 302 at the DAF. The building was modeled as described in the Curie benchmark.[5] It is only concrete with no opening. Air was also modeled,[5] but the Godiva-IV framework, the Comet framework, and crane were neglected. Gaps in the Godiva-IV model were filled with air. ENDF/B-VIII.0 data were used for the concrete building and the air, but ENDF/B-VII.1 data were used for Godiva-IV, as in Secs. II, III, IV, and V. Results from the modified model are shown in Table VI. k_{eff} increased by 506 ± 1 pcm from the result shown in Table I. Comparing Table VI with Table I shows that moving to Building 302 while decreasing the separation distance, decreasing the size of the safety block, and increasing the spindle glory hole diameter causes a very slight softening of the neutron spectrum within Godiva-IV.

Table VI. Godiva-IV Results in Building 302 and Using Smaller Separation, Smaller Safety Block, Larger Glory Hole, and Production Release of ENDF/B-VII.1.

Parameter		Value
k_{eff}		0.99623 ± 0.00001
ANEF		1.4251 MeV
EALF		0.78941 MeV
Fraction of fissions caused by neutrons in energy range	thermal	0.05 %
	intermediate	5.52 %
	fast	94.43 %
Fission conversion factor[(a)]		3.364E+4 ± 0.05%

(a) (Fissions in Godiva-IV)/[(Fissions in foil)/(g ^{235}U in foil)].

The flux spectrum in the fission foil in the modified model is compared with the flux spectrum in the fission foil in HEU-MET-FAST-086 (Sec. II) in Figure 9. The spectra in the top figure are very similar, but the bottom figure shows the difference, modified model minus HEU-MET-FAST-086 (note this is absolute, not relative). As in Figure 1, the largest differences occur around 3 MeV, and the relative difference is about the same as in Figure 1.

The flux spectra are compared for point detector 1 in Figure 10. The building causes a very long low-energy tail. The spectra at the other two point detectors (not shown) are similar.

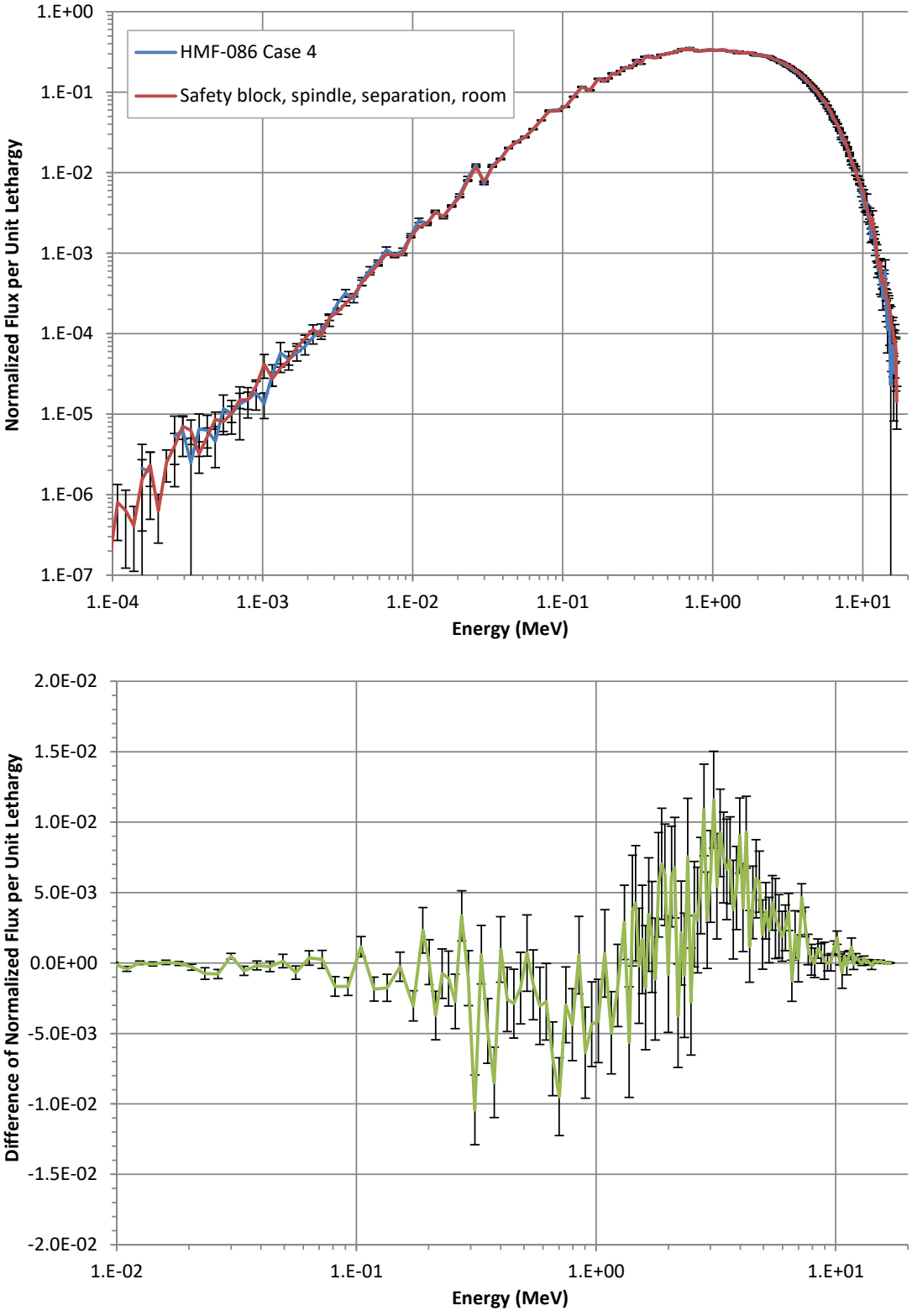

Figure 9. Comparison of neutron flux spectra in the fission foil between HEU-MET-FAST-086 and Godiva-IV in Building 302 and using smaller separation, smaller safety block, larger glory hole, and production release of ENDF/B-VII.1.

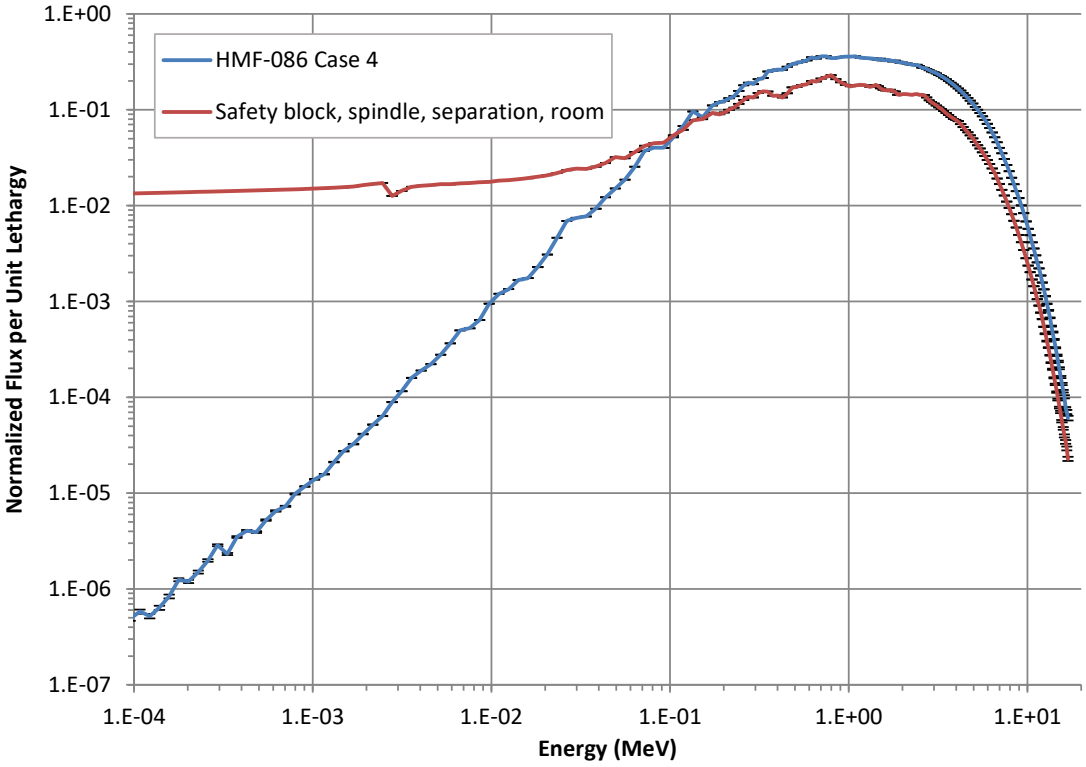

Figure 10. Comparison of neutron flux spectra at point detector 1 between HEU-MET-FAST-086 and Godiva-IV in Building 302 and using smaller separation, smaller safety block, larger glory hole, and production release of ENDF/B-VII.1.

VII. ENDF/B-VIII.0

The calculations of Secs. II through VI used ENDF/B-VII.1 nuclear data for Godiva-IV for consistency with HEU-MET-FAST-086. In this section, the calculations of Sec. V were repeated with ENDF/B-VIII.0 nuclear data. Results are shown in Table VII. k_{eff} increased by 37 ± 1 pcm from the result shown in Table V. Comparing Table VII with Table V shows an interesting case in which ANEF decreases but EALF increases. The energy distribution of neutrons causing fission suggests a slight hardening of the spectrum due to ENDF/B-VIII.0 nuclear data.

Table VII. Godiva-IV Results Using Smaller Separation, Smaller Safety Block, Larger Glory Hole, and Production Release of ENDF/B-VIII.0.

Parameter		Value
k_{eff}		0.99607 ± 0.00001
ANEF		1.4241 MeV
EALF		0.80589 MeV
Fraction of fissions caused by neutrons in energy range	thermal	0.00 %
	intermediate	5.02 %
	fast	94.98 %
Fission conversion factor[(a)]		3.356E+4 ± 0.05%

(a) (Fissions in Godiva-IV)/[(Fissions in foil)/(g ^{235}U in foil)].

The flux spectrum in the fission foil in the model with ENDF/B-VIII.0 nuclear data is compared with the flux spectrum in the fission foil in the model with ENDF/B-VII.1 nuclear data (Sec. V) in Figure 11. The spectra in the top figure are very similar, but the bottom figure shows the difference, the model with ENDF/B-VIII.0 minus the model with ENDF/B-VII.1 (note this is absolute, not relative). There are four areas with noticeable differences. The spectrum in the model with ENDF/B-VIII.0 is larger at ~0.3 MeV and ~1.2 MeV, but smaller at ~0.6 MeV and ~3 MeV.

The flux spectra are compared for the three point detectors in Figure 12, Figure 13, and Figure 14. The differences are similar to those in the fission foil (Figure 11). The model with ENDF/B-VIII.0 has a slightly smaller low-energy tail.

Thus, within the fission foil, using ENDF/B-VIII.0 for Godiva-IV induces changes in the flux spectrum similar in size to the changes due to using smaller separation, a smaller safety block, and a larger glory hole. At the point detectors, using ENDF/B-VIII.0 induces changes in the flux spectrum much larger than those due to changing the model.

ENDF/B-VIII.0 data were also used in the baseline model, HEU-MET-FAST 086 Case 4 of Sec. II. The change in k_{eff} from the value of Table I was also 37 ± 1 pcm. The fraction of fissions caused by neutrons in the three energy ranges were the same as in Table VII.

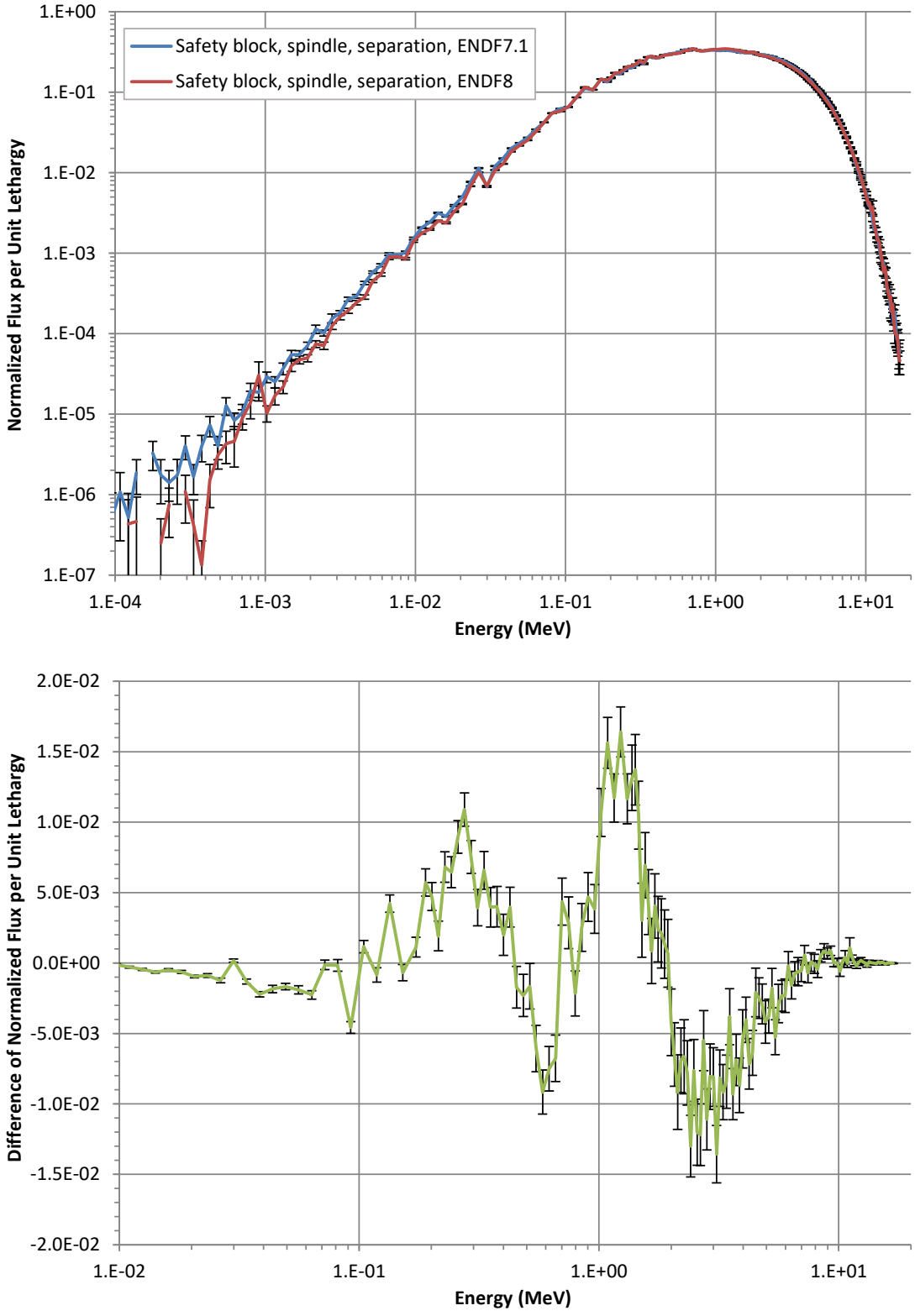

Figure 11. Comparison of neutron flux spectra in the fission foil between ENDF/B-VII.1 and ENDF/B-VIII.0 for Godiva-IV using smaller separation, smaller safety block, and larger glory hole.

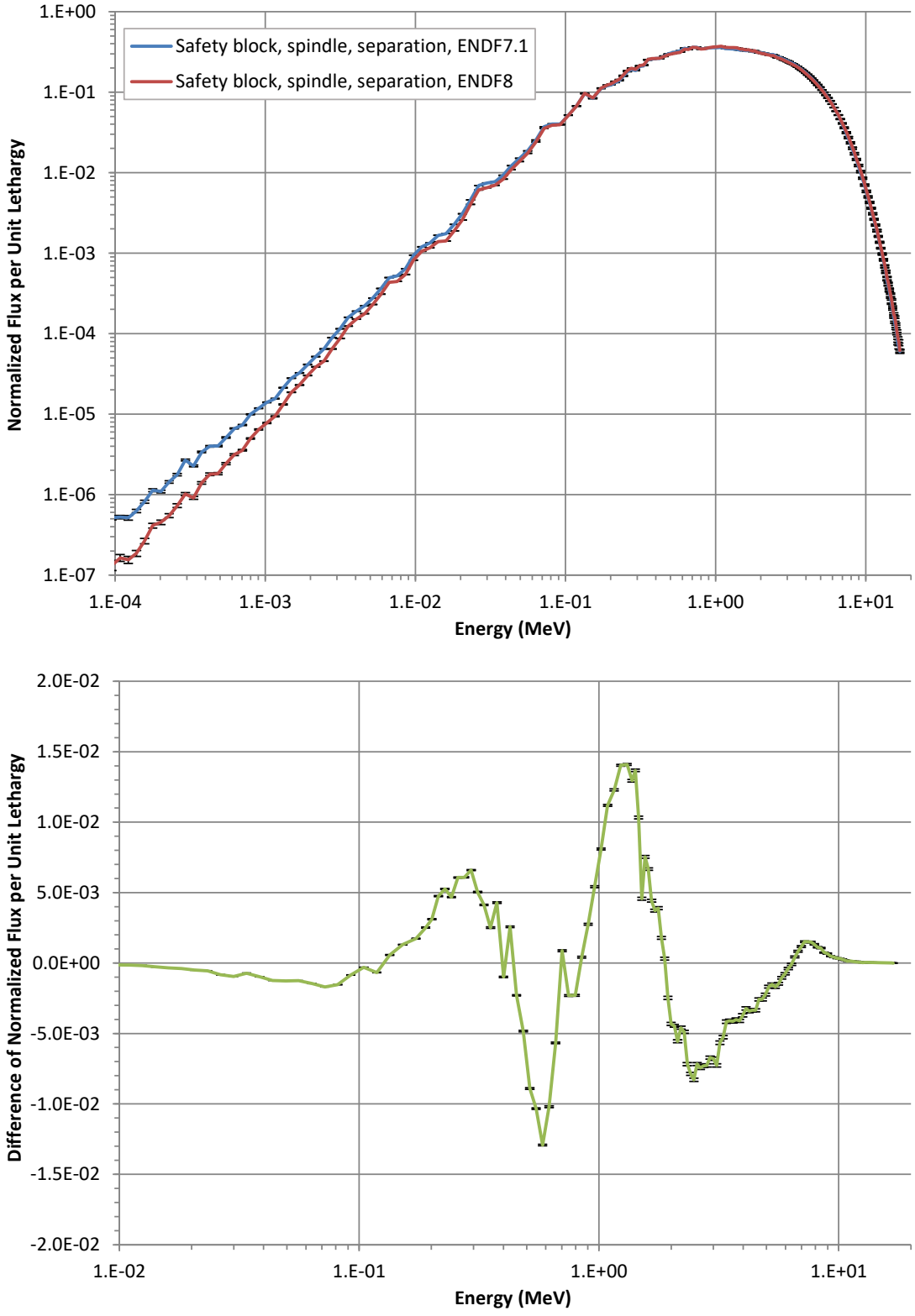

Figure 12. Comparison of neutron flux spectra at point detector 1 between ENDF/B-VII.1 and ENDF/B-VIII.0 for Godiva-IV using smaller separation, smaller safety block, and larger glory hole.

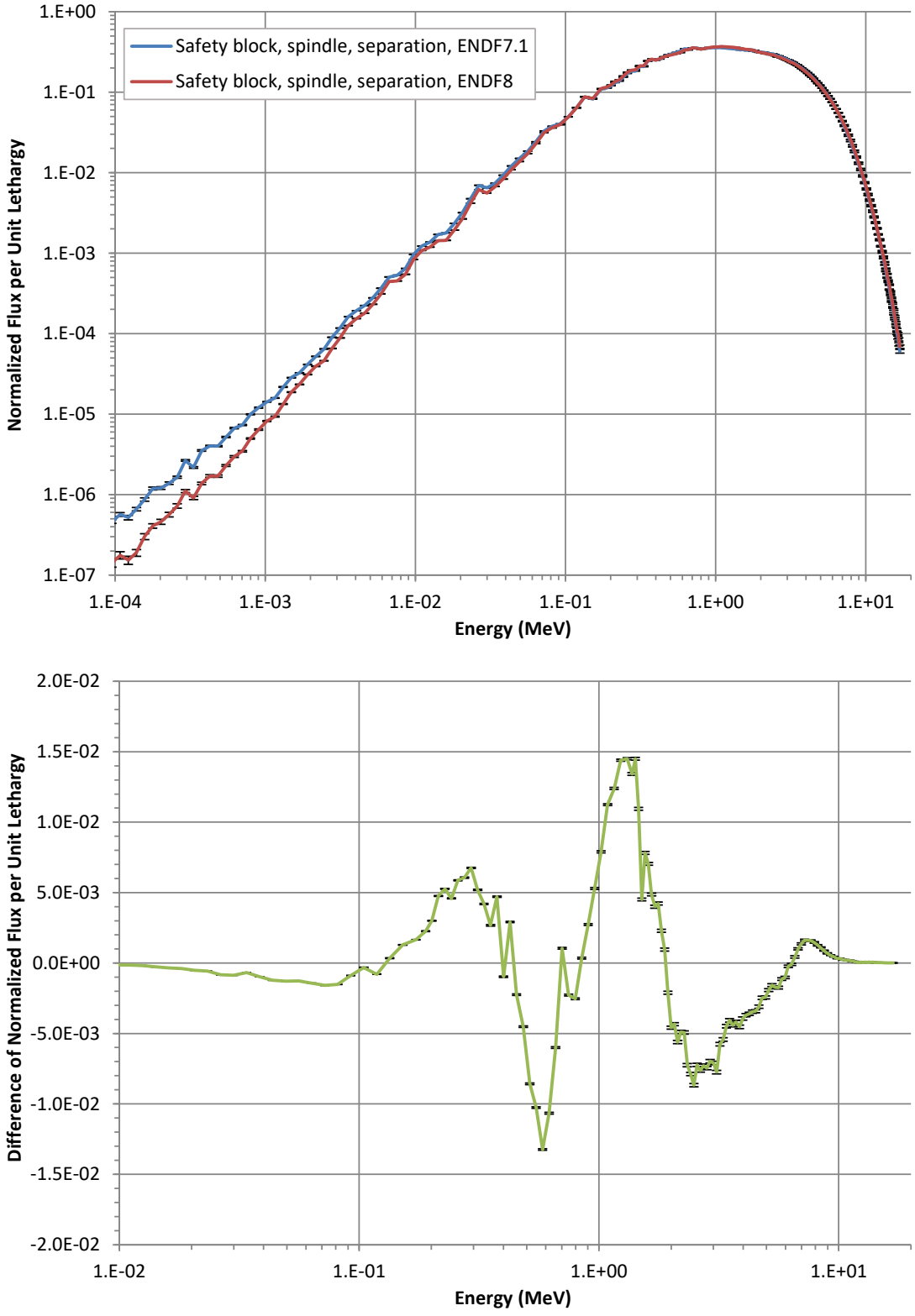

Figure 13. Comparison of neutron flux spectra at point detector 2 between ENDF/B-VII.1 and ENDF/B-VIII.0 for Godiva-IV using smaller separation, smaller safety block, and larger glory hole.

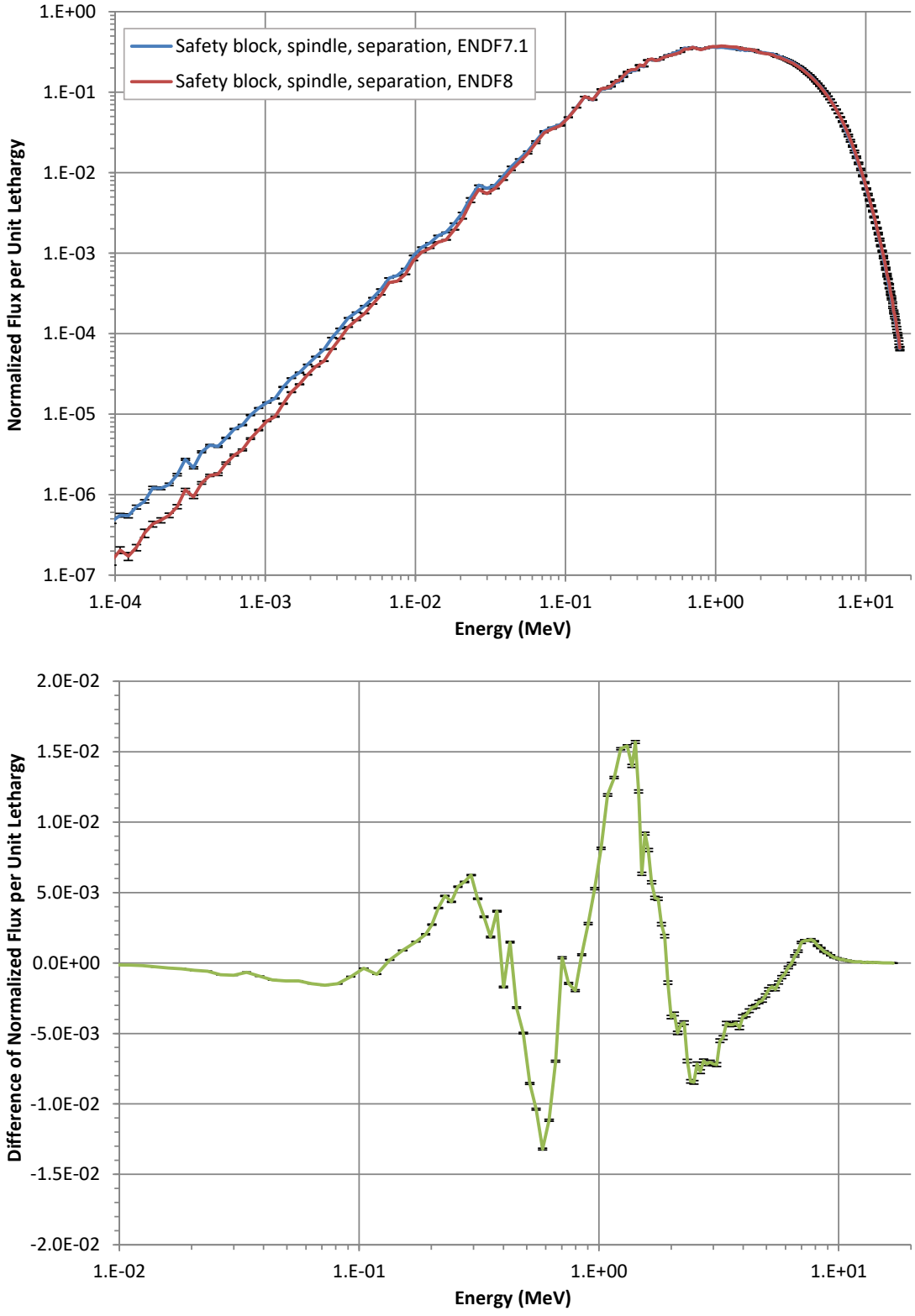

Figure 14. Comparison of neutron flux spectra at point detector 3 between ENDF/B-VII.1 and ENDF/B-VIII.0 for Godiva-IV using smaller separation, smaller safety block, and larger glory hole.

VIII. Summary and Conclusions

This report has estimated reactivity and spectral parameter changes in Godiva-IV due to the following updates to the benchmark model of HEU-MET-FAST-086 Case 4:

1. Use production release of ENDF/B-VII.1.
2. #1 and increase diameter of glory hole in spindle.
3. #2 and decrease height of safety block while increasing its density.
4. #3 and decrease separation between safety block and inner subassembly plate.
5. #4 and include air and Building 302.

In addition, the models of #1 and #4 were run with ENDF/B-VIII.0 nuclear data.

The change in k_{eff} for each modification and the cumulative effect are shown in Table VIII.

Table VIII. Cumulative Effect of Modifications to HEU-MET-FAST-086 Case 4 (Each Modification Includes the Preceding Modifications).[(a)]

Modification	$\Delta k_{eff} \pm 1\sigma_{MC}$ (Difference from Preceding Modification)	$\Delta k_{eff} \pm 1\sigma_{MC}$ (Difference from Benchmark Model, Cumulative)
Increase diameter of glory hole in spindle	-	–0.00062 ± 0.00001
Decrease height of safety block while increasing its density	0.00143 ± 0.00001	0.00081 ± 0.00001
Decrease separation between safety block and inner subassembly plate	0.00372 ± 0.00001	0.00453 ± 0.00001
Include air and Building 302	0.00053 ± 0.00001	0.00506 ± 0.00001

(a) The base case is the high-precision calculation using the production release of ENDF/B-VII.1 discussed in Sec. II.

The two modifications mentioned in the errata prepended to HEU-MET-FAST-086, item #3 in the list above, together cause k_{eff} to increase by 81 ± 1 pcm from the benchmark value. The neutron spectral parameters change only slightly. The benchmark with those modifications is essentially identical to the existing benchmark.

Incorporating the decreased separation between the safety block and the inner subassembly plate with the previous modifications causes the largest increase in k_{eff}, 372 ± 1 pcm, a cumulative increase of 453 ± 1 pcm from the benchmark value. The flux spectrum within the assembly softens slightly, but the flux spectra at external detectors is altered only very slightly.

Incorporating the air, walls, floor, and ceiling of Building 302 with the previous modifications causes k_{eff} to increase by 53 ± 1 pcm, a cumulative increase of 509 ± 1 pcm from the benchmark value. The flux spectrum within the assembly softens slightly, but the flux spectra at external point detectors changes dramatically, developing a very long low-energy tail.

Using ENDF/B-VIII.0 nuclear data in model #4 causes k_{eff} to increase by 37 ± 1 pcm, a cumulative increase of 490 ± 1 pcm from the benchmark value. Other than including the air and Building 302, this is the change that had the largest effect on the flux spectra at external point detectors. In fact, changing to ENDF/B-VIII.0 caused an even larger change than including Building 302 in the fraction of fissions

caused by neutrons in the intermediate and fast energy ranges. Using ENDF/B-VIII.0 nuclear data had a similar effect on the baseline model, HEU-MET-FAST-086 Case 4.

In summary, the corrections to the benchmark model cause a large increase in k_{eff} (450 to 550 pcm, depending on whether the building is included and what cross sections are used), but the changes to the neutron flux spectrum are small compared to those caused by using the latest nuclear data. In general, however, spectral effects are minimal except for the addition of Building 302.

An update to the Godiva-IV benchmark, HEU-MET-FAST-086, will incorporate the changes described in #1 through #4 above. Due to the even larger effect of the room, a new case or cases will be evaluated and compared to current control rod positions at delayed critical in Building 302 at the DAF.

Acknowledgments

The author would like to thank Travis Smith, Geordie McKenzie, Victoria Hagopian, and Joetta Goda (LANL NEN-2), who began updating the Godiva-IV model.

References

1. Russell D. Mosteller, Joetta Goda, Nicolas Authier, Nichole Ellis, and Bruce Patton, "Godiva-IV Delayed-Critical Experiments and Description of an Associated Prompt-Burst Experiment," *International Handbook of Evaluated Criticality Safety Benchmark Experiments*, HEU-MET-FAST-086, Revision 0, Nuclear Energy Agency, Organization for Economic Co-Operation and Development (2014).

2. Christopher J. Werner, ed., "MCNP® User's Manual, Code Version 6.2," Los Alamos National Laboratory report LA–UR–17–29981, Rev. 0 (Oct. 27, 2017).

3. D. P. Hickman, D. P. Heinrichs, R. Hudson, C. Wong, D. Ward, C. Wilson, L. Clark, F. Trompier, and J. Goda, "Dosimetry Characterization of the Godiva Reactor Under Burst Conditions," Lawrence Livermore National Laboratory report LLNL-TR-729408 (June 22, 2017).

4. https://xweb.lanl.gov/projects/data/nuclear/ndi_data/transport/group_structs/lanl_hifi.html.

5. Jeffrey A. Favorite, Theresa Cutler, Travis Grove, Kelsey Amundson, and Jesse Norris, "Intermediate-Spectrum Critical Assemblies with a Polytetrafluoroethylene-HEU Core Surrounded by a Copper Reflector," *International Handbook of Evaluated Criticality Safety Benchmark Experiments*, HEU-MET-INTER-011, Revision 0, Nuclear Energy Agency, Organization for Economic Co-Operation and Development, in preparation (2022).

JAF:jaf

Distribution:
J. T. Goorley, XCP-7, MS A143, jgoorley@lanl.gov
K. M. Amundson, NEN-2, MS B228, kamundson@lanl.gov
T. E. Cutler, NEN-2, MS B228, tcutler@lanl.gov
J. M. Goda, NEN-2, MS B228, jgoda@lanl.gov
T. J. Grove, NEN-2, MS B228, tgove@lanl.gov
D. K. Hayes, NEN-2, MS B228, dkayes@lanl.gov
J. D. Hutchinson, NEN-2, MS B228, jesson@lanl.gov
G. E. McKenzie, NEN-2, MS B228, gmckenzie@lanl.gov
A. T. McSpaden, NEN-2, MS B228, mcspaden@lanl.gov
T. A. Smith, NEN-2, MS B228, traviss@lanl.gov
R. C. Little, XCP-3, MS F663, rcl@lanl.gov
J. L. Alwin, XCP-7, MS A143, jalwin@lanl.gov
J. A. Favorite, XCP-7, MS F663, fave@lanl.gov
National Security Research Center, nsrc-cataloging@lanl.gov
XCP-7 File

Appendix A
Computing the Fission Conversion Factor

The fission conversion factor is used to convert the measured (more appropriately, the *inferred from measurements*) number of fissions in a foil per gram of ^{235}U in the foil to the number of fissions in the Godiva-IV HEU parts. Thus, the fission conversion factor must be calculated as the total number of fissions in the Godiva-IV HEU parts divided by the number of fissions in the foil per gram of ^{235}U in the foil. The delayed-critical models of this report are assumed to be in steady state, so fission reaction rates were used instead of the number of fissions.

Track-length tallies of the fission reaction rate were computed for each HEU material specified in the Godiva-IV model. The total fission rates, rather than the volume averages, were computed. The sum of these fission rates is the total fission rate in the Godiva-IV HEU parts.

In the fission foil, however, a track-length tally of the volume-average fission reaction rate was computed. The result of this tally is the fission rate per volume of foil. Dividing by the mass density of ^{235}U in the foil gives the fission rate per unit mass of ^{235}U in the foil.

To be even more specific, the MCNP6.2 input lines that compute these tallies are as follows:

```
f4:n 98
fc4 U235 Foil Tally (average)
fm4 (-1 10 -6)
f14:n (3 4 5 6)
sd14 1.
fc14 Inner Subassembly Plate Tally
fm14 (-1 7 -6)
f24:n 7
sd24 1.
fc24 Safety Block Tally
fm24 (-1 6 -6)
f34:n (14 15 16 17 18 19 20 21)
sd34 1.
fc34 Fuel Ring Tally
fm34 (-1 5 -6)
f44:n (25 26 27 31 32 33)
sd44 1.
fc44 Control Rod Tally
fm44 (-1 8 -6)
f54:n (36 37 38)
sd54 1.
fc54 Burst Rod Tally
fm54 (-1 9 -6)
```

The F4 tally is for the volume-average fission rate in the foil, cell 98 with material 10 (i.e., fissions/s in foil per cm^3 foil). The F14, F24, F34, F44, and F54 tallies are the volume-total (note SD 1. cards) fission rates in the Godiva-IV HEU materials (i.e., fissions/s in Godiva fuel). The Godiva fission conversion factor C_{Godiva} in (fissions/s in Godiva)/[(fissions/s in foil)/(g ^{235}U in foil)] is

$$C_{Godiva} = \frac{(\mathrm{F14}+\mathrm{F24}+\mathrm{F34}+\mathrm{F44}+\mathrm{F54})}{\mathrm{F4}} \times 17.35365, \qquad \text{(A.1)}$$

where the density of ^{235}U in the foil is 18.5994 (g foil)/(cm^3 foil) × 0.933022 (g ^{235}U)/(g foil) = 17.35365 (g ^{235}U in foil)/(cm^3 foil) (see Sec. II).

In the models of Secs. III, IV, V, VI, and VII, the fission foil has diameter 0.5 inches, thickness 0.00248 cm, density 18.5994 g/cm^3, and ^{235}U concentration 93.3022 wt%. In the model of Sec. II, the glory hole in the spindle is smaller, so the fission foil's diameter is 0.2220 inches. Otherwise, the fission foil is the same as in the other sections.

In the models of Secs. III, IV, V, VI, and VII, the fission foil is at the bottom of an aluminum sample holder whose inner and outer diameters are 0.505 and 0.552 inches, respectively. The bottom end is 0.026965 inches thick, the top end is 0.700787 inches thick, and the overall length is 5.249701 inches. The bottom of the sample holder is 0.144 inches from the bottom of the inner subassembly plate. The material is pure ^{27}Al at a density of 2.62524 g/cm^3. In the model of Sec. II, the glory hole in the spindle is smaller, so the sample holder's inner and outer diameters are 0.224245 and 0.245116 inches, respectively. Otherwise, the sample holder is the same as in the other sections.

The spindle glory hole diameter in the benchmark model of Sec. II is too small. The fission foil and sample holder diameters in the other models are realistic. The fission foil and sample holder diameters in the benchmark model of Sec. II were scaled to the fractional cross-sectional area of the glory hole in the modified models. In other words, the cross-sectional area of the component in the benchmark model divided by the cross-sectional area of the glory hole in the benchmark model is equal to the cross-sectional area of the component in the modified model divided by the cross-sectional area of the glory hole in the modified model.

Appendix B
Input File Listings

MCNP6.2 Input File for HEU-MET-FAST-086 Case 4 with Production Release of ENDF/B-VII.1 Nuclear Data (Sec. II)

```
Godiva-IV  HEU-MET-FAST-086  Case 4 DC  BR Out  LDN Masses BMark Model ENDF/B-VII.1
c  Core
c  Spindle
1        1    0.088296      1   -2    4   -5          $ Spindle
2        1    0.088296      2   69  -85  -86          $ Nut on Spindle
c  Homogenized Inner Subassembly Plate
3        7    0.047627      2   -7    8   -9          $ Bottom of ISP
4        7    0.047627      2   -6    9  -11          $ Lower Middle of ISP
5        7    0.047627      2   -7   11  -12          $ Upper Middle of ISP
6        7    0.047627     10   -7   12  -13          $ Top of ISP
c  Safety Block
7        6    0.047100      2  -14   16  -15          $ Cylindrical Safety Block
c  Safety Block Base
8        1    0.088296    -17   19  -20               $ SB Base Bottom
9        1    0.088296    -16  -18   20               $ SB Base Wide
10       1    0.088296     -2  -15   16               $ SB Base Top
c  Notches for Homogenized Fuel Ring
11       0                -24   30  -31   34  -35
                           36  #57                    $ Right Notch
12       0                -24   30  -31  -37  -39
                           40  #58                    $ Front Left Notch
13       0                -24   30  -31  -38  -41
                           42  #59                    $ Back Left Notch
c  Homogenized Fuel Ring
14       5    0.047622    -24   25   26   27   28
                           62  -29  #11  #12  #13
                          #57  #58  #59               $ Btm Outer Annulus
15       5    0.047622     22   28  -29  -61
                           25   26   27               $ Btm Inner Annulus
16       5    0.047622     -9   22  -24   25   26
                           27   29  #11  #12  #13
                          #57  #58  #59               $ Lower Middle Annulus
17       5    0.047622      9   21  -24   25   26
                           27  -31  #11  #12  #13
                          #57  #58  #59               $ Middle Annulus
18       5    0.047622    -11   21  -24   31
                          #11  #12  #13  #57  #58
                          #59                         $ Lower Center Annulus
19       5    0.047622     11   22  -24  -32  #11
                          #12  #13
                          #57  #58  #59               $ Upper Center Annulus
20       5    0.047622     22   32  -33  -64          $ Inner Top Annulus
21       5    0.047622    -24   32  -33   65
                          #11  #12  #13
                          #57  #58  #59               $ Outer Top Annulus
c  Control and Burst Rods
22       0                -25   59  -31               $ Hole above Control Rod 1
23       0                -25   44   51  -59          $ Gap between CR1 & Rings
24       0                -43   57  -59               $ Top Hole in CR1
25       8    0.048437     43  -44   51  -54          $ Bottom Region, CR1
26       8    0.048437    -44   54  -57               $ Solid Middle Region, CR1
27       8    0.048437     43  -44   57  -59          $ Top Region, CR1
28       0                -27   60  -31               $ Hole above Control Rod 2
29       0                -27   48   52  -60          $ Gap between CR2 & Rings
30       0                -47   58  -60               $ Top Hole in CR2
31       8    0.048437     47  -48   52  -55          $ Bottom Region, CR2
32       8    0.048437    -48   55  -58               $ Solid Middle Region, CR2
33       8    0.048437     47  -48   58  -60          $ Top Region, CR2
34       0                -26  -31   56               $ Hole above Burst Rod
35       0                -26   46   28  -56          $ Gap between BR & Rings
36       9    0.049553     45  -46   49  -50          $ Bottom Region, Burst Rod
37       9    0.049553    -46   50  -53               $ Middle Region, BR
38       9    0.049553     45  -46   53  -56          $ Top Region, Burst Rod
39       0                -45   53  -56               $ Cylinder, BR Pin
```

```
40       0                -43   51  -54              $ Bottom Hole, CR1
41       0                -47   52  -55              $ Bottom Hole, CR2
42       0                -45   49  -50              $ Bottom Hole, Burst Rod
c  Support-Pad Ring and Bearing Ring
43       2    0.086010    -29   61  -62   63
                           25   26   27              $ Support-Pad Ring
44       2    0.086010     32   64  -65  -66         $ Solid Bearing Ring
c  Subassembly Cover Plate
45       0                 3   13  -67  -69         $ Central Hole in SCP
46       0                13  -22   67  -68         $ Inner Void in SCP
47       2    0.086010     22   33  -23  -69         $ Edge of SCP
48       2    0.086010    -22   67   68  -69         $ Center of SCP
c  Mounting Plate
49       0                -70   74  -75              $ Empty Central Hole
50       0                 25  -71   74  -75         $ Empty Hole for CR1
51       0                 26  -72   74  -75         $ Empty Hole for Burst Rod
52       0                 27  -73   74  -75         $ Empty Hole for CR2
53       4    0.058593     70   71   72   73   74
                          -75  -87                   $ Mounting Plate
c  Clamp Supports (Legs)
54       1    0.088296     75  -76   77  -78   79
                          -80                       $ Rectangular Right Leg
55       like 54 but trcl (0 0 0  -0.5 -0.8660254 0
                            -0.8660254 -0.5 0  0 0 1) $ Front Bolt for FL Leg
56       like 54 but trcl (0 0 0  -0.5  0.8660254 0
                            -0.8660254  0.5 0  0 0 1) $ Front Bolt for BL Leg
c  Clamps
57       3    0.083675     34  -35  -79
                           63  -66   84              $ Middle of Clamp Back
58       like 57 but trcl (0 0 0  -0.5 -0.8660254 0
                            -0.8660254 -0.5 0  0 0 1) $ Middle of Clamp Back
59       like 57 but trcl (0 0 0  -0.5  0.8660254 0
                            -0.8660254  0.5 0  0 0 1) $ Middle of Clamp Back
60       3    0.083675     34  -35  -63  -79   81
                           83                       $ Bottom Prong, Back Leg
61       like 60 but trcl (0 0 0  -0.5 -0.8660254 0
                            -0.8660254 -0.5 0  0 0 1) $ Bottom Prong, FL Leg
62       like 60 but trcl (0 0 0  -0.5  0.8660254 0
                            -0.8660254  0.5 0  0 0 1) $ Bottom Prong, FL Leg
63       3    0.083675     34  -35  -79  -82   66
                           83                       $ Top Prong, Back Leg
64       like 63 but trcl (0 0 0  -0.5 -0.8660254 0
                            -0.8660254 -0.5 0  0 0 1) $ Top Prong, FL Leg
65       like 63 but trcl (0 0 0  -0.5  0.8660254 0
                            -0.8660254  0.5 0  0 0 1) $ Top Prong, FL Leg
c  Outer Void Regions
66       0                 17   19  -20  -22       $ Cyl Gap below Platform
67       0                -16   18   20  -22       $ Gap outside Platform
68       0                  7    8   -9  -22
69       0                  6    9  -11  -21       $ Fuel Annulus / ISP Gap
c  Inner Void Regions
70       0                  5  -82  -87
                          #63  #64  #65
71       0                 -5   24   75  -87   88
                           89  #54  #57  #60  #63  $ BR Void above Mntg Plate
72       0                 -5   24   75  -87  -88
                           89  #54  #57  #60  #63  $ FR Void above Mntg Plate
73       0                 -5   24   75  -87  -88
                          -89  #55  #58  #61  #64  $ FL Void above Mntg Plate
74       0                 -5   24   75  -87   88
                          -89  #56  #59  #62  #65  $ BL Void above Mntg Plate
75       0                 23   33  -64  -69       $ Gap between SCP and BRing
76       0                -25   74  -51            $ Void below Control Rod 1
77       0                -27   74  -52            $ Void below Control Rod 2
78       0                -26   74  -49            $ Hole below Burst Rod
79       0                -26  -28   46   49       $ Void around Burst Rod
80       0                 22  -24   25   26   27
                          -63   75  #60  #61  #62  $ Void below Sup Pad Cyl
81       0                -24   25   26   27  -28
                           62   63  #57  #58  #59  $ Void Sup Pad Cyl
82       0                 22   25   26   27  -28
                          -61   63                 $ Void inside Sup Pad Cyl
83       0                -19  -22   75            $ Void below Sfty Blk Base
```

```
84       0                 22  -64  -66   69       $ Void inside Bearing Ring
85       0                 22  -24   33   65  -66  $ Void outside Bearing Ring
                          #57  #58  #59             $ Void outside Bearing Ring
86       0                 -5   22  -24   66
                          #63  #64  #65             $ Void above Bearing Ring
87       0                 -8   14   16  -22
88       0                  7   11  -13  -22       $ Upr ISP / Fuel Ring Gap
89       0                  2   -5  -22   69   #2  $ Spindle / Fuel Ring Gap
90       0                  2   -3   12  -69       $ Gap around Spindle
91       0                 -8  -14   15
92       0                 -2   -4    8           $ Space below Spindle
93       0                 -1    4   -5           $ Lower Glory Hole
94       0                  3  -10   12  -13       $ ISP - Spindle Gap
c  External Void Regions
95       0                 82
96       0                -82   74   87
97       0                -74

c  Surfaces for Spindle
1     cz   0.31750                              $ Glory-Hole Radius
2     cz   1.27000                              $ Spindle Bottom Middle OR
3     cz   1.42875                              $ Spindle Top Middle OR
4     pz   0.00254                              $ Bottom of Spindle
5     pz  11.43254                              $ Top of Spindle
c  Surfaces for Intermediate Inner Subassembly Plate
6     cz   3.92430                              $ OR of Inner Sub Plate
7     cz   4.38150                              $ OR of Lower Inner Sub Plate
8     pz   0.0                                  $ Bottom of Inner Sub Plate
9     pz   2.54000                              $ Top of ISP Wide Region
10    cz   3.50520                              $ Upper IR of ISP
11    pz   4.96570                              $ Top of ISP Indentation
12    pz   6.98754                              $ Bottom of ISP Inner Annulus
13    pz   7.64794                              $ Top of Innerr Sub Plate
c  Surfaces for Safety Block
14    cz   4.29260                              $ Safety Block Outer Radius
15    pz  -0.25400                              $ Top of Safety Block
16    pz  -7.85128                              $ Bottom of Safety Block
c  Surfaces for Safety Block Base
17    cz   2.45000                              $ OR of SB Base Middle
18    cz   3.65760                              $ OR of SB Base Platform
19    pz -12.81320                              $ Bottom of SB Base
20    pz  -9.30148                              $ Bottom of SB Base Platform
c  Surfaces for Fuel Rings
21    cz   3.97510                              $ Smaller IR of Fuel Ring
22    cz   4.44500                              $ Larger IR of Fuel Ring
23    cz   5.08000                              $ IR of Sup Pad Slot
24    cz   8.89000                              $ OR of FuelRing
25    c/z  3.33375   -5.774224   1.11125        $ FR Hole, Control or Burst Rod
26    c/z -6.66750    0.0        1.11125        $ Lt Hole, Control or Burst Rod
27    c/z  3.33375    5.774224   1.11125        $ BR Hole, Control or Burst Rod
28    pz  -7.80455                              $ Bottom of Ring
29    pz  -7.43839                              $ Bottom of Ring Slot
30    pz  -4.89458                              $ Bottom of Ring Outer Edge
31    pz   4.64820                              $ Top of Ring Outer Edge
32    pz   7.27160                              $ Bottom of Bearing Ring
33    pz   7.78416                              $ Top of Fuel Ring
34    py  -1.11125                              $ Front Edge of Left Notch
35    py   1.11125                              $ Back Edge of Left Notch
36    px   8.49376                              $ Back Edge of Left Notch
37    p    1.0        1.7320508  0.0 -16.9857200 $ Back Edge, BL Notch
38    p    1.0       -1.7320508  0.0 -16.9857200 $ Back Edge, BR Notch
39    p    1.7320508 -1.0        0.0   1.9247415 $ Lower Edge, BL Notch
40    p    1.7320508 -1.0        0.0  -1.9247415 $ Upper Edge, BL Notch
41    p    1.7320508  1.0        0.0   1.9247415 $ Lower Edge, BR Notch
42    p    1.7320508  1.0        0.0  -1.9247415 $ Upper Edge, BR Notch
c  Surfaces for Control Rods and Burst Rod
43    c/z  3.33375   -5.774224   0.47625        $ Control Rod 1 IR
44    c/z  3.33375   -5.774224   1.09220        $ Control Rod 1 OR
45    c/z -6.66750    0.0        0.47625        $ Burst Rod IR
46    c/z -6.66750    0.0        1.09220        $ Burst Rod OR
47    c/z  3.33375    5.774224   0.47625        $ Control Rod 2 IR
48    c/z  3.33375    5.774224   1.09220        $ Control Rod 2 OR
49    pz -18.34007                              $ Bottom of Burst Rod (Full Out)
```

```
50    pz -16.43507                              $ Top of Burst Rod Bottom Hole
51    pz -10.86933                              $ Bottom of Control Rod 1
52    pz -10.81405                              $ Bottom of Control Rod 2
53    pz  -8.81507                              $ Flat Bottom of BR Top Hole
54    pz  -8.96493                              $ Top of CR1 Bottom Hole
55    pz  -8.90905                              $ Top of CR2 Bottom Hole
56    pz  -5.64007                              $ Top of Burst Rod (Full Out)
57    pz  -0.07493                              $ Bottom of CR1 Top Hole
58    pz  -0.01905                              $ Bottom of CR2 Top Hole
59    pz   1.83007                              $ Top of Control Rod 1
60    pz   1.88595                              $ Top of Control Rod 2
c  Surfaces for Support-Pad Ring
61    cz   5.71695                              $ Inner Radius of Supt Pad Cyl
62    cz   7.29488                              $ Outer Radius of Supt Pad Cyl
63    pz  -9.02589                              $ Bottom of Support Pad Cyl
c  Surfaces for Bearing Ring
64    cz   5.08381                              $ Inner Radius of Bearing Ring
65    cz   7.29615                              $ Outer Radius of Bearing Ring
66    pz   8.75411                              $ Top of Bearing Ring
c  Surfaces for Subassembly Cover Plate
67    cz   1.43510                              $ Radius of Central Hole in SCP
68    pz   8.00680                              $ Top of SCP Raised Edge
69    pz   8.32430                              $ Top of Subassembly Cvr Plate
c  Surfaces for Mounting Plate
70    cz   5.23875                              $ Radius of Central Hole in MP
71    c/z  3.33375   -5.774224   1.27000        $ FR Hole for Control Rod 1
72    c/z -6.66750    0.0        1.27000        $ Left Hole for Burst Rod
73    c/z  3.33375    5.774224   1.27000        $ BR Hole for Control Rod 2
74    pz  -20.37715                             $ Bottom of Mounting Plate
75    pz  -16.56715                             $ Top of Mounting Plate
c  Surfaces for Clamp Support (Leg)
76    pz    4.38785                             $ Top of Right Leg
77    py   -1.42875                             $ Front Edge of Right Leg
78    py    1.42875                             $ Back Edge of Right Leg
79    px   12.94130                             $ Right Edge of Right Leg Inset
80    px   18.94130                             $ Right Edge of Right Leg
c  Surfaces for Clamp
81    pz  -12.67587                             $ Bottom of Clamp
82    pz   12.40409                             $ Top of Clamp
83    px    5.08000                             $ Left Edge of Prongs
84    px    8.49630                             $ Left Edge of Clamp Back
c  Surfaces for Nuts and Bolts
85    cz    2.22250                             $ OR for Nut on Spindle
86    pz    9.59430                             $ Top of Nut on Spindle
c
87    cz   44.45                                $ Otr Radius of Mounting Plate
88    py    0.0
89    px    0.0
c
94 pz 0.43425    $ Sample Holder Bottom

mode     n
idum 1
rand gen=2 seed=110000001
kcode 4e6 1.0 100 1200
imp:n    1.0    93r    0.0     2r
ksrc     0.0    0.0   -1.0
c        SS 303  (8.0 g/cc)
m1 6000.80c 3.0083e-4
        14028.80c 1.5821e-3
        14029.80c 8.0109e-5
        14030.80c 5.3177e-5
        15031.80c 1.5554e-4
c        16000.62c 4.5067e-4
        16032.80c 4.28226634e-4 16033.80c 3.380025e-6
        16034.80c 1.8973207e-5  16036.80c 9.0134e-8
        24050.80c 7.2466e-4 24052.80c 1.3974e-2
        24053.80c 1.5844e-3 24054.80c 3.9443e-4
        25055.80c 8.7693e-4
        26054.80c 3.5742e-3 26056.80c 5.5564e-2
        26057.80c 1.2722e-3 26058.80c 1.6962e-4
        28058.80c 5.0437e-3 28060.80c 1.9282e-3
        28061.80c 8.3482e-5 28062.80c 2.6522e-4
```

```
        28064.80c 6.7229e-5
c        42000.66c 1.5065e-4
        42092.80c 2.235646e-5  42094.80c 1.3935125e-5
        42095.80c 2.398348e-5  42096.80c 2.512842e-5
        42097.80c 1.4387075e-5 42098.80c 3.6351845e-5
        42100.80c 1.4507595e-5
c        SAE 4340  (7.85 g/cc)
m2 6000.80c 1.5940e-3
        14028.80c 3.4929e-4 14029.80c 1.7686e-5
        14030.80c 1.1740e-5
        15031.80c 2.7472e-5
c        16000.62c 2.9481e-5
        16032.80c 2.80128462e-5 16033.80c 2.211075e-7
        16034.80c 1.2411501e-6  16036.80c 5.8962e-9
        24050.80c 3.1603e-5 24052.80c 6.0944e-4
        24053.80c 6.9097e-5 24054.80c 1.7202e-5
        25055.80c 6.2385e-4
        26054.80c 4.7824e-3 26056.80c 7.4345e-2
        26057.80c 1.7022e-3 26058.80c 2.2696e-4
        28058.80c 9.8985e-4 28060.80c 3.7842e-4
        28061.80c 1.6384e-5 28062.80c 5.2051e-5
        28064.80c 1.3194e-5
c        42000.66c 1.2319e-4
        42092.80c 1.8281396e-5 42094.80c 1.1395075e-5
        42095.80c 1.9611848e-5 42096.80c 2.0548092e-5
        42097.80c 1.1764645e-5 42098.80c 2.9725747e-5
        42100.80c 1.1530584e-5
c        VascoMax 300  (8.0 g/cc)
m3 6000.80c 8.0221e-5
        13027.80c 1.7855e-4
        14028.80c 7.9104e-5 14029.80c 4.0054e-6
        14030.80c 2.6588e-6
        15031.80c 7.7770e-6
c        16000.62c 7.5112e-6
        16032.80c 7.13714224e-6 16033.80c 5.6334e-8
        16034.80c 3.1622152e-7  16036.80c 1.50224e-9
c        22000.62c 7.3453e-4
        22046.80c 5.8762400E-05 22047.80c 5.3620690E-05
        22048.80c 5.4208314E-04 22049.80c 4.0399150E-05
        22050.80c 3.9664620E-05
        25055.80c 4.3847e-5
        26054.80c 3.4070e-3 26056.80c 5.2965e-2
        26057.80c 1.2127e-3 26058.80c 1.6169e-4
        27059.80c 7.1938e-3
        28058.80c 1.0367e-2 28060.80c 3.9635e-3
        28061.80c 1.7160e-4 28062.80c 5.4518e-4
        28064.80c 1.3819e-4
c        42000.66c 2.4103e-3
        42092.80c 3.5768852e-4 42094.80c 2.2295275e-4
        42095.80c 3.8371976e-4 42096.80c 4.0203804e-4
        42097.80c 2.3018365e-4 42098.80c 5.8160539e-4
        42100.80c 2.3211189e-4
c        Pure Aluminum
m4 13027.80c 5.8593e-2
c        HEU + Mo (93.15 wt.% for Homogenized Ring)
m5 42092.80c 2.527252e-4  42094.80c 1.575275e-4
        42095.80c 2.711176e-4  42096.80c 2.840604e-4
        42097.80c 1.626365e-4  42098.80c 4.109339e-4
        42100.80c 1.639989e-4
c        42000.66c 1.7030e-3
        92233.80c 4.6343e-6 92234.80c 4.7016e-4
        92235.80c 4.2801e-2 92236.80c 3.1112e-4
        92238.80c 2.3328e-3
c        HEU + Mo (93.17 wt.% for Safety Block)
m6 42092.80c 1.6916116e-4  42094.80c 1.0544075e-4
        42095.80c 1.8147208e-4 42096.80c 1.9013532e-4
        42097.80c 1.0886045e-4 42098.80c 2.7505787e-4
        42100.80c 1.0977237e-4
c        42000.66c 1.1399e-3
        92233.80c 4.6384e-6 92234.80c 4.7068e-4
        92235.80c 4.2848e-2 92236.80c 3.1140e-4
        92238.80c 2.3253e-3
c        HEU + Mo (93.16 wt.% for Homogenized ISP)
```

```
m7 42092.80c 2.5596032e-4 42094.80c 1.59544e-4
        42095.80c 2.7458816e-4 42096.80c 2.8769664e-4
        42097.80c 1.9471840e-4 42098.80c 4.1619424e-4
        42100.80c 1.6609824e-4
c        42000.66c 1.7248e-3
        92233.80c 4.6326e-6 92234.80c 4.7007e-4
        92235.80c 4.2791e-2 92236.80c 3.1101e-4
        92238.80c 2.3249e-3
c        HEU + Mo (93.16 wt.% for Control Rods 1 and 2)
m8 42092.80c 2.30762e-4 42094.80c 1.438375e-4
        42095.80c 2.4755600e-4 42096.80c 2.5937400e-4
        42097.80c 1.4850250e-4 42098.80c 3.7522150e-4
        42100.80c 1.4974650e-4
c        42000.66c 1.5550e-3
        92233.80c 4.7315e-6 92234.80c 4.8008e-4
        92235.80c 4.3703e-2 92236.80c 3.1765e-4
        92238.80c 2.3767e-3
c        HEU + Mo (93.16 wt.% for Burst Rod)
m9 42092.80c 2.3608956e-4 42094.80c 1.4715825e-4
        42095.80c 2.5327128e-4 42096.80c 2.6536212e-4
        42097.80c 1.5193095e-4 42098.80c 3.8388417e-4
        42100.80c 1.5320367e-4
c        42000.66c 1.5909e-3
        92233.80c 4.8405e-6 92234.80c 4.9114e-4
        92235.80c 4.4710e-2 92236.80c 3.2497e-4
        92238.80c 2.4314e-3
c
totnu
prdmp     j   575
print -30
```

MCNP6.2 Input File for HEU-MET-FAST-086 Case 4 with Smaller Separation, Smaller Safety Block, Larger Glory Hole, and Production Release of ENDF/B-VIII.0 (Sec. VII)

```
Godiva-IV HEU-MET-FAST-086 Case 4 DC BR Out LDN Masses
c TAS added SB shim, fixed SB position, modified safty block density using proportions from the amount
of volume lost over time
c this is essential becasue the assumed mass was measured in the 2000s and the volume was assumed from
orignal drawings
c TAS changed SB shim to 1018 steel (correct material), updated cross sections to .80c
c mod 8 by TAS corrects the CR1 bottom hole to have the proper depth
c mod 9 by JAF preserves the original mass of the safety block by decreasing the density
c mod 10 by JAF decreases the separation distance of safety block from 0.1 in. to 0.0160 in.
c
c Core
c Spindle
1 1 0.088296 90 -2 4 -5 $ Spindle
2 1 0.088296 2 69 -85 -86 $ Nut on Spindle
c Homogenized Inner Subassembly Plate
3 7 0.047627 2 -7 8 -9 $ Bottom of ISP
4 7 0.047627 2 -6 9 -11 $ Lower Middle of ISP
5 7 0.047627 2 -7 11 -12 $ Upper Middle of ISP
6 7 0.047627 10 -7 12 -13 $ Top of ISP
c Safety Block
7 6 0.047738 2 -14 100 -15 $ Cylindrical Safety Block
c Safety Block Base
8 1 0.088296 -17 19 -20 $ SB Base Bottom
9 1 0.088296 -16 -18 20 $ SB Base Wide
10 1 0.088296 -2 -15 16 $ SB Base Top
102 11 -7.87 2 -101 -100 16 $ SB Shim
c Notches for Homogenized Fuel Ring
11 0 -24 30 -31 34 -35 36 #57 $ Right Notch
12 0 -24 30 -31 -37 -39 40 #58 $ Front Left Notch
13 0 -24 30 -31 -38 -41 42 #59 $ Back Left Notch
c Homogenized Fuel Ring
14 5 0.047622 -24 25 26 27 28 62 -29 #11 #12 #13 #57 #58 #59 $ Btm Outer Annulus
15 5 0.047622 22 28 -29 -61 25 26 27 $ Btm Inner Annulus
16 5 0.047622 -9 22 -24 25 26 27 29 #11 #12 #13 #57 #58 #59 $ Lower Middle Annulus
17 5 0.047622 9 21 -24 25 26 27 -31 #11 #12 #13 #57 #58 #59 $ Middle Annulus
18 5 0.047622 -11 21 -24 31 #11 #12 #13 #57 #58 #59 $ Lower Center Annulus
19 5 0.047622 11 22 -24 -32 #11 #12 #13 #57 #58 #59 $ Upper Center Annulus
```

```
20 5 0.047622 22 32 -33 -64 $ Inner Top Annulus
21 5 0.047622 -24 32 -33 65 #11 #12 #13 #57 #58 #59 $ Outer Top Annulus
c Control and Burst Rods
22 0 -25 59 -31 $ Hole above Control Rod 1
23 0 -25 44 51 -59 $ Gap between CR1 & Rings
24 0 -43 57 -59 $ Top Hole in CR1
25 8 0.048437 43 -44 51 -54 $ Bottom Region, CR1
26 8 0.048437 -44 54 -57 $ Solid Middle Region, CR1
27 8 0.048437 43 -44 57 -59 $ Top Region, CR1
28 0 -27 60 -31 $ Hole above Control Rod 2
29 0 -27 48 52 -60 $ Gap between CR2 & Rings
30 0 -47 58 -60 $ Top Hole in CR2
31 8 0.048437 47 -48 52 -55 $ Bottom Region, CR2
32 8 0.048437 -48 55 -58 $ Solid Middle Region, CR2
33 8 0.048437 47 -48 58 -60 $ Top Region, CR2
34 0 -26 -31 56 $ Hole above Burst Rod
35 0 -26 46 28 -56 $ Gap between BR & Rings
36 9 0.049553 45 -46 49 -50 $ Bottom Region, Burst Rod
37 9 0.049553 -46 50 -53 $ Middle Region, BR
38 9 0.049553 45 -46 53 -56 $ Top Region, Burst Rod
39 0 -45 53 -56 $ Cylinder, BR Pin
40 0 -43 51 -54 $ Bottom Hole, CR1
41 0 -47 52 -55 $ Bottom Hole, CR2
42 0 -45 49 -50 $ Bottom Hole, Burst Rod
c Support-Pad Ring and Bearing Ring
43 2 0.086010 -29 61 -62 63 25 26 27 $ Support-Pad Ring
44 2 0.086010 32 64 -65 -66 $ Solid Bearing Ring
c Subassembly Cover Plate
45 0 3 13 -67 -69 $ Central Hole in SCP
46 0 13 -22 67 -68 $ Inner Void in SCP
47 2 0.086010 22 33 -23 -69 $ Edge of SCP
48 2 0.086010 -22 67 68 -69 $ Center of SCP
c Mounting Plate
49 0 -70 74 -75 $ Empty Central Hole
50 0 25 -71 74 -75 $ Empty Hole for CR1
51 0 26 -72 74 -75 $ Empty Hole for Burst Rod
52 0 27 -73 74 -75 $ Empty Hole for CR2
53 4 0.058593 70 71 72 73 74 -75 -87 $ Mounting Plate
c Clamp Supports (Legs)
54 1 0.088296 75 -76 77 -78 79 -80 $ Rectangular Right Leg
55 like 54 but trcl (0 0 0 -0.5 -0.8660254 0 -0.8660254 -0.5 0 0 0 1) $ Front Bolt for FL Leg
56 like 54 but trcl (0 0 0 -0.5 0.8660254 0 -0.8660254 0.5 0 0 0 1) $ Front Bolt for BL Leg
c Clamps
57 3 0.083675 34 -35 -79 63 -66 84 $ Middle of Clamp Back
58 like 57 but trcl (0 0 0 -0.5 -0.8660254 0 -0.8660254 -0.5 0 0 0 1) $ Middle of Clamp Back
59 like 57 but trcl (0 0 0 -0.5 0.8660254 0 -0.8660254 0.5 0 0 0 1) $ Middle of Clamp Back
60 3 0.083675 34 -35 -63 -79 81 83 $ Bottom Prong, Back Leg
61 like 60 but trcl (0 0 0 -0.5 -0.8660254 0 -0.8660254 -0.5 0 0 0 1) $ Bottom Prong, FL Leg
62 like 60 but trcl (0 0 0 -0.5 0.8660254 0 -0.8660254 0.5 0 0 0 1) $ Bottom Prong, FL Leg
63 3 0.083675 34 -35 -79 -82 66 83 $ Top Prong, Back Leg
64 like 63 but trcl (0 0 0 -0.5 -0.8660254 0 -0.8660254 -0.5 0 0 0 1) $ Top Prong, FL Leg
65 like 63 but trcl (0 0 0 -0.5 0.8660254 0 -0.8660254 0.5 0 0 0 1) $ Top Prong, FL Leg
c Outer Void Regions
66 0 17 19 -20 -22 $ Cyl Gap below Platform
67 0 -16 18 20 -22 $ Gap outside Platform
68 0 7 8 -9 -22
69 0 6 9 -11 -21 $ Fuel Annulus / ISP Gap
c Inner Void Regions
70 0 5 -82 -87 #63 #64 #65
71 0 -5 24 75 -87 88 89 #54 #57 #60 #63 $ BR Void above Mntg Plate
72 0 -5 24 75 -87 -88 89 #54 #57 #60 #63 $ FR Void above Mntg Plate
73 0 -5 24 75 -87 -88 -89 #55 #58 #61 #64 $ FL Void above Mntg Plate
74 0 -5 24 75 -87 88 -89 #56 #59 #62 #65 $ BL Void above Mntg Plate
75 0 23 33 -64 -69 $ Gap between SCP and BRing
76 0 -25 74 -51 $ Void below Control Rod 1
77 0 -27 74 -52 $ Void below Control Rod 2
78 0 -26 74 -49 $ Hole below Burst Rod
79 0 -26 -28 46 49 $ Void around Burst Rod
80 0 22 -24 25 26 27 -63 75 #60 #61 #62 $ Void below Sup Pad Cyl
81 0 -24 25 26 27 -28 62 63 #57 #58 #59 $ Void Sup Pad Cyl
82 0 22 25 26 27 -28 -61 63 $ Void inside Sup Pad Cyl
83 0 -19 -22 75 $ Void below Sfty Blk Base
84 0 22 -64 -66 69 $ Void inside Bearing Ring
```

```
85 0 22 -24 33 65 -66 #57 #58 #59 $ Void outside Bearing Ring
86 0 -5 22 -24 66 #63 #64 #65 $ Void above Bearing Ring
87 0 -8 14 16 -22 $ Void outside SB
88 0 7 11 -13 -22 $ Upr ISP / Fuel Ring Gap
89 0 2 -5 -22 69 #2 $ Spindle / Fuel Ring Gap
90 0 2 -3 12 -69 $ Gap around Spindle
91 0 -8 -14 15 $ Void above SB
92 0 -2 -4 8 $ Space below Spindle
c 93 0 -1 4 -5 $ Lower Glory Hole
94 0 3 -10 12 -13 $ ISP - Spindle Gap
103 0 -14 101 -100 16 $ Void near SB shim
97 0 -90 4 -91 $ Glory Hole thru hole
98 0 -90 91 -5 $ Glory Hole corrected
c External Void Regions
99 0 82
100 0 -82 74 87
101 0 -74

c Surfaces for Spindle
1 cz 0.31750 $ OLD Glory-Hole Radius
2 cz 1.27000 $ Spindle Bottom Middle OR
3 cz 1.42875 $ Spindle Top Middle OR
4 pz 0.00254 $ Bottom of Spindle
5 pz 11.43254 $ Top of Spindle
c Surfaces for Intermediate Inner Subassembly Plate
6 cz 3.92430 $ OR of Inner Sub Plate
7 cz 4.38150 $ OR of Lower Inner Sub Plate
8 pz 0.0 $ Bottom of Inner Sub Plate
9 pz 2.54000 $ Top of ISP Wide Region
10 cz 3.50520 $ Upper IR of ISP
11 pz 4.96570 $ Top of ISP Indentation
12 pz 6.98754 $ Bottom of ISP Inner Annulus
13 pz 7.64794 $ Top of Innerr Sub Plate
c Surfaces for Safety Block
14 cz 4.29260 $ Safety Block Outer Radius
15 pz -0.04064 $ Top of Safety Block
100 pz -7.53632 $ Bottom of Safety Block
16 pz -7.63792 $ Bottom of Safety Block Shim
101 cz 4.0005 $ OR of safety block shim
c Surfaces for Safety Block Base
17 cz 2.45000 $ OR of SB Base Middle
18 cz 3.65760 $ OR of SB Base Platform
19 pz -12.59980 $ Bottom of SB Base
20 pz -9.08812 $ Bottom of SB Base Platform
c Surfaces for Fuel Rings
21 cz 3.97510 $ Smaller IR of Fuel Ring
22 cz 4.44500 $ Larger IR of Fuel Ring
23 cz 5.08000 $ IR of Sup Pad Slot
24 cz 8.89000 $ OR of FuelRing
25 c/z 3.33375 -5.774224 1.11125 $ FR Hole, Control or Burst Rod
26 c/z -6.66750 0.0 1.11125 $ Lt Hole, Control or Burst Rod
27 c/z 3.33375 5.774224 1.11125 $ BR Hole, Control or Burst Rod
28 pz -7.80455 $ Bottom of Ring
29 pz -7.43839 $ Bottom of Ring Slot
30 pz -4.89458 $ Bottom of Ring Outer Edge
31 pz 4.64820 $ Top of Ring Outer Edge
32 pz 7.27160 $ Bottom of Bearing Ring
33 pz 7.78416 $ Top of Fuel Ring
34 py -1.11125 $ Front Edge of Left Notch
35 py 1.11125 $ Back Edge of Left Notch
36 px 8.49376 $ Back Edge of Left Notch
37 p 1.0 1.7320508 0.0 -16.9857200 $ Back Edge, BL Notch
38 p 1.0 -1.7320508 0.0 -16.9857200 $ Back Edge, BR Notch
39 p 1.7320508 -1.0 0.0 1.9247415 $ Lower Edge, BL Notch
40 p 1.7320508 -1.0 0.0 -1.9247415 $ Upper Edge, BL Notch
41 p 1.7320508 1.0 0.0 1.9247415 $ Lower Edge, BR Notch
42 p 1.7320508 1.0 0.0 -1.9247415 $ Upper Edge, BR Notch
c Surfaces for Control Rods and Burst Rod
43 c/z 3.33375 -5.774224 0.47625 $ Control Rod 1 IR
44 c/z 3.33375 -5.774224 1.09220 $ Control Rod 1 OR
45 c/z -6.66750 0.0 0.47625 $ Burst Rod IR
46 c/z -6.66750 0.0 1.09220 $ Burst Rod OR
47 c/z 3.33375 5.774224 0.47625 $ Control Rod 2 IR
```

```
48 c/z 3.33375 5.774224 1.09220 $ Control Rod 2 OR
49 pz -18.34007 $ Bottom of Burst Rod (Full Out)
50 pz -16.43507 $ Top of Burst Rod Bottom Hole
51 pz -10.86993 $ Bottom of Control Rod 1
52 pz -10.81405$ Bottom of Control Rod 2
53 pz -7.54507 $ Flat Bottom of BR Top Hole
54 pz -8.96493 $ Top of CR1 Bottom Hole
55 pz -8.90905 $ Top of CR2 Bottom Hole
56 pz -5.64007 $ Top of Burst Rod (Full Out)
57 pz -0.07493 $ Bottom of CR1 Top Hole
58 pz -0.01905 $ Bottom of CR2 Top Hole
59 pz 1.83007 $ Top of Control Rod 1
60 pz 1.88595 $ Top of Control Rod 2
c Surfaces for Support-Pad Ring
61 cz 5.71695 $ Inner Radius of Supt Pad Cyl
62 cz 7.29488 $ Outer Radius of Supt Pad Cyl
63 pz -9.02589 $ Bottom of Support Pad Cyl
c Surfaces for Bearing Ring
64 cz 5.08381 $ Inner Radius of Bearing Ring
65 cz 7.29615 $ Outer Radius of Bearing Ring
66 pz 8.75411 $ Top of Bearing Ring
c Surfaces for Subassembly Cover Plate
67 cz 1.43510 $ Radius of Central Hole in SCP
68 pz 8.00680 $ Top of SCP Raised Edge
69 pz 8.32430 $ Top of Subassembly Cvr Plate
c Surfaces for Mounting Plate
70 cz 5.23875 $ Radius of Central Hole in MP
71 c/z 3.33375 -5.774224 1.27000 $ FR Hole for Control Rod 1
72 c/z -6.66750 0.0 1.27000 $ Left Hole for Burst Rod
73 c/z 3.33375 5.774224 1.27000 $ BR Hole for Control Rod 2
74 pz -20.37715 $ Bottom of Mounting Plate
75 pz -16.56715 $ Top of Mounting Plate
c Surfaces for Clamp Support (Leg)
76 pz 4.38785 $ Top of Right Leg
77 py -1.42875 $ Front Edge of Right Leg
78 py 1.42875 $ Back Edge of Right Leg
79 px 12.94130 $ Right Edge of Right Leg Inset
80 px 18.94130 $ Right Edge of Right Leg
c Surfaces for Clamp
81 pz -12.67587 $ Bottom of Clamp
82 pz 12.40409 $ Top of Clamp
83 px 5.08000 $ Left Edge of Prongs
84 px 8.49630 $ Left Edge of Clamp Back
c Surfaces for Nuts and Bolts
85 cz 2.22250 $ OR for Nut on Spindle
86 pz 9.59430 $ Top of Nut on Spindle
c
87 cz 44.45 $ Otr Radius of Mounting Plate
88 py 0.0
89 px 0.0
c
90 cz 0.71501 $ Glory Hole Radius
91 pz 0.36576 $ Glory Hole Bottom

mode n
idum 1
rand gen=2 seed=510000001
kcode 4e6 1.0 100 1200
imp:n 1.0 96r 0.0 2r
ksrc 0.0 0.0 -1.0
c SS 303 (8.0 g/cc)
m1 6012.00c 2.9752E-04 6013.00c 3.3091E-06
        14028.00c 1.5821e-3
        14029.00c 8.0109e-5
        14030.00c 5.3177e-5
        15031.00c 1.5554e-4
c        16000.62c 4.5067e-4
        16032.00c 4.28226634e-4 16033.00c 3.380025e-6
        16034.00c 1.8973207e-5  16036.00c 9.0134e-8
        24050.00c 7.2466e-4 24052.00c 1.3974e-2
        24053.00c 1.5844e-3 24054.00c 3.9443e-4
        25055.00c 8.7693e-4
        26054.00c 3.5742e-3 26056.00c 5.5564e-2
```

```
        26057.00c 1.2722e-3 26058.00c 1.6962e-4
        28058.00c 5.0437e-3 28060.00c 1.9282e-3
        28061.00c 8.3482e-5 28062.00c 2.6522e-4
        28064.00c 6.7229e-5
c        42000.66c 1.5065e-4
        42092.00c 2.235646e-5  42094.00c 1.3935125e-5
        42095.00c 2.398348e-5  42096.00c 2.512842e-5
        42097.00c 1.4387075e-5 42098.00c 3.6351845e-5
        42100.00c 1.4507595e-5
c SAE 4340 (7.85 g/cc)
m2 6012.00c 1.5765E-03 6013.00c 1.7534E-05
        14028.00c 3.4929e-4 14029.00c 1.7686e-5
        14030.00c 1.1740e-5
        15031.00c 2.7472e-5
c        16000.62c 2.9481e-5
        16032.00c 2.80128462e-5 16033.00c 2.211075e-7
        16034.00c 1.2411501e-6  16036.00c 5.8962e-9
        24050.00c 3.1603e-5 24052.00c 6.0944e-4
        24053.00c 6.9097e-5 24054.00c 1.7202e-5
        25055.00c 6.2385e-4
        26054.00c 4.7824e-3 26056.00c 7.4345e-2
        26057.00c 1.7022e-3 26058.00c 2.2696e-4
        28058.00c 9.8985e-4 28060.00c 3.7842e-4
        28061.00c 1.6384e-5 28062.00c 5.2051e-5
        28064.00c 1.3194e-5
c        42000.66c 1.2319e-4
        42092.00c 1.8281396e-5 42094.00c 1.1395075e-5
        42095.00c 1.9611848e-5 42096.00c 2.0548092e-5
        42097.00c 1.1764645e-5 42098.00c 2.9725747e-5
        42100.00c 1.1530584e-5
c VascoMax 300 (8.0 g/cc)
m3 6012.00c 7.9339E-05 6013.00c 8.8243E-07
        13027.00c 1.7855e-4
        14028.00c 7.9104e-5 14029.00c 4.0054e-6
        14030.00c 2.6588e-6
        15031.00c 7.7770e-6
c        16000.62c 7.5112e-6
        16032.00c 7.13714224e-6 16033.00c 5.6334e-8
        16034.00c 3.1622152e-7  16036.00c 1.50224e-9
c        22000.62c 7.3453e-4
        22046.00c 5.8762400E-05 22047.00c 5.3620690E-05
        22048.00c 5.4208314E-04 22049.00c 4.0399150E-05
        22050.00c 3.9664620E-05
        25055.00c 4.3847e-5
        26054.00c 3.4070e-3 26056.00c 5.2965e-2
        26057.00c 1.2127e-3 26058.00c 1.6169e-4
        27059.00c 7.1938e-3
        28058.00c 1.0367e-2 28060.00c 3.9635e-3
        28061.00c 1.7160e-4 28062.00c 5.4518e-4
        28064.00c 1.3819e-4
c        42000.66c 2.4103e-3
        42092.00c 3.5768852e-4 42094.00c 2.2295275e-4
        42095.00c 3.8371976e-4 42096.00c 4.0203804e-4
        42097.00c 2.3018365e-4 42098.00c 5.8160539e-4
        42100.00c 2.3211189e-4
c Pure Aluminum
m4 13027.00c 5.8593e-2
c HEU + Mo (93.15 wt.% for Homogenized Ring)
m5 42092.00c 2.527252e-4  42094.00c 1.575275e-4
        42095.00c 2.711176e-4  42096.00c 2.840604e-4
        42097.00c 1.626365e-4  42098.00c 4.109339e-4
        42100.00c 1.639989e-4
c        42000.66c 1.7030e-3
        92233.00c 4.6343e-6 92234.00c 4.7016e-4
        92235.00c 4.2801e-2 92236.00c 3.1112e-4
        92238.00c 2.3328e-3
c HEU + Mo (93.17 wt.% for Safety Block)
m6 42092.00c 1.6916116e-4  42094.00c 1.0544075e-4
        42095.00c 1.8147208e-4 42096.00c 1.9013532e-4
        42097.00c 1.0886045e-4 42098.00c 2.7505787e-4
        42100.00c 1.0977237e-4
c    42000.66c 1.1399e-3
        92233.00c 4.6384e-6 92234.00c 4.7068e-4
```

```
        92235.00c 4.2848e-2 92236.00c 3.1140e-4
        92238.00c 2.3253e-3
c HEU + Mo (93.16 wt.% for Homogenized ISP)
m7 42092.00c 2.5596032e-4 42094.00c 1.59544e-4
        42095.00c 2.7458816e-4 42096.00c 2.8769664e-4
        42097.00c 1.9471840e-4 42098.00c 4.1619424e-4
        42100.00c 1.6609824e-4
c        42000.66c 1.7248e-3
        92233.00c 4.6326e-6 92234.00c 4.7007e-4
        92235.00c 4.2791e-2 92236.00c 3.1101e-4
        92238.00c 2.3249e-3
c HEU + Mo (93.16 wt.% for Control Rods 1 and 2)
m8 42092.00c 2.30762e-4 42094.00c 1.438375e-4
        42095.00c 2.4755600e-4 42096.00c 2.5937400e-4
        42097.00c 1.4850250e-4 42098.00c 3.7522150e-4
        42100.00c 1.4974650e-4
c        42000.66c 1.5550e-3
        92233.00c 4.7315e-6 92234.00c 4.8008e-4
        92235.00c 4.3703e-2 92236.00c 3.1765e-4
        92238.00c 2.3767e-3
c HEU + Mo (93.16 wt.% for Burst Rod)
m9 42092.00c 2.3608956e-4 42094.00c 1.4715825e-4
        42095.00c 2.5327128e-4 42096.00c 2.6536212e-4
        42097.00c 1.5193095e-4 42098.00c 3.8388417e-4
        42100.00c 1.5320367e-4
c        42000.66c 1.5909e-3
        92233.00c 4.8405e-6 92234.00c 4.9114e-4
        92235.00c 4.4710e-2 92236.00c 3.2497e-4
        92238.00c 2.4314e-3
c SB Shim 1018 steel (7.87 g/cc)
m11 6012.00c -1.7786E-01 6013.00c -2.1436E-03
        25055.00c -0.08 15031.00c -0.04
        16032.00c -0.04751  16033.00c -0.000375
        16034.00c -0.002105 16036.00c -0.00001
        26054.00c -5.7797   26056.00c -91.39898
        26057.00c -2.1923   26058.00c -0.27902
c
totnu
print -30
```